

AD-A054 173

GEORGIA INST OF TECH ATLANTA SCHOOL OF AEROSPACE ENG--ETC F/G 21/5  
NOISE SUPPRESSION IN JET INLETS.(U)  
FEB 78 B ZINN, W L MEYER, W A BELL

UNCLASSIFIED

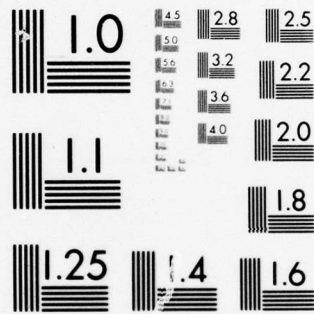
AFOSR-TR-78-0696

F49620-77-C-0066  
NL

| OF |  
AD  
A054173



END  
DATE  
FILMED  
6 -78  
DDC



MICROCOPY RESOLUTION TEST CHART  
NATIONAL BUREAU OF STANDARDS-1963-A

AFOSR-TR- 78 - 0696

AFOSR Interim Scientific Report

AFOSR-TR-

AD A 054173

AD No. 00000000  
DDC FILE COPY

NOISE SUPPRESSION IN JET INLETS

Prepared for

Air Force Office of Scientific Research  
Director of Aerospace Sciences

Bolling AFB, D. C.

by

Ben T. Zinn

William L. Meyer

William A. Bell

School of Aerospace Engineering  
Georgia Institute of Technology  
Atlanta, Georgia 30332



Approved for public release; distribution unlimited

AFOSR Contract No. F49620-77-C-0066

February 1978

Conditions of Reproduction

Reproduction, translation, publication, use and disposal in whole or in part by or for the United States Government is permitted.

AFOSR Interim Scientific Report

AFOSR-TR-

NOISE SUPPRESSION IN JET INLETS

Prepared for

Air Force Office of Scientific Research  
Director of Aerospace Sciences

Bolling AFB, D. C.

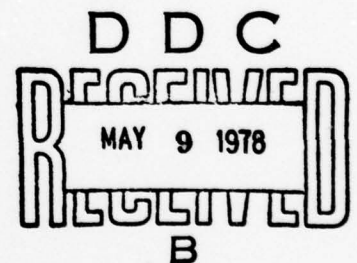
by

Ben T. Zinn

William L. Meyer

William A. Bell

School of Aerospace Engineering  
Georgia Institute of Technology  
Atlanta, Georgia 30332



Approved for public release; distribution unlimited

AFOSR Contract No. F49620-77-C-0066

February 1978

Conditions of Reproduction

Reproduction, translation, publication, use and disposal in whole or in part by or for the United States Government is permitted.

# ABSTRACT

This report summarizes the work performed during the first year of a research effort to determine the sound fields associated with jet engine inlet configurations. A solution approach for axisymmetric bodies based upon the integral formulation of the wave equation has been developed. This solution approach circumvents the uniqueness problems which normally occur at certain frequencies when "straight forward" solutions of the integral equation are obtained. A numerical method and a computer program for solving for the acoustic field associated with general inlet configurations and boundary conditions have also been developed. To evaluate the numerical method, computed and exact results are compared for a sphere and a finite length cylinder. For continuous boundary conditions, the agreement is within ten per cent over a range of nondimensional frequencies from one to ten. For discontinuous boundary conditions, the numerical errors increase by a factor of two. This report presents results for a given inlet configuration and the computed and exact solutions are shown to agree to within ten per cent over the nondimensional frequency range from one to ten.

ACCESSION for		
NTIS	White Section	<input checked="" type="checkbox"/>
DDC	B-N Section	<input type="checkbox"/>
UNANNOUNCED		<input type="checkbox"/>
JUSTIFICATION		
BY		
DISTRIBUTION/AVAILABILITY CODES		
Dist.	AVAIL	and/or SPECIAL
A		

## I. INTRODUCTION

This report summarizes the results obtained during the first year of support under AFOSR Contract Number F49620-77-C-0066. This contract was initiated on February 1, 1977.

The research conducted under this contract is directed towards developing analytical techniques for predicting the characteristics of the radiated sound fields from jet engine inlets. Such capabilities are necessary to evaluate the effectiveness of potential sound source modifications and the efficiency of sound suppression techniques for fan and compressor noise attenuation in inlets. During the first year, the conducted research efforts have concentrated on the development of an efficient analytical technique for the prediction of the radiated fields associated with lined inlet configurations. In the second year, experimental investigations will be conducted to provide data for comparison with the theoretical predictions.

During the first year, a solution approach based upon an integral formulation of the wave equation has been developed and used to determine the characteristics of the sound fields of several previously investigated geometries. Efficient numerical techniques have been devised for solving the integral equation, and the necessary computer programs have been written and tested. These programs are now capable of computing the surface and radiated sound fields for arbitrary geometries with lined or unlined surfaces and sound sources of arbitrary spatial dependence. These capabilities are necessary for the investigations of sound fields from jet inlet configurations.

The efforts conducted under this contract has resulted in three publications<sup>1,2,3</sup> which are included in Appendices A-C of this report. These publications provide more detailed descriptions of the research efforts conducted

under this contract. The research performed during the first year is summarized in the following sections.

## II. ANALYTICAL TECHNIQUE

The general analytical method used to determine the radiated sound fields from arbitrary geometries is described in Appendix A. This technique is based on the integral form of the solutions to the wave equation. This general formulation has been specialized to axisymmetric configurations, which are applicable to jet engine configurations which are of interest in this study, in Appendix B.

The study of sound radiation involves the determination of the acoustic field over an infinite domain. However, with the integral formulation of the wave equation, the acoustic potential, which is proportional to the acoustic pressure, can be computed at any point in the far field solely from the values of the potential distribution at the surface. Thus, the problem is reduced to solving for the acoustic field at the surface only instead of over an infinite domain.

Several problems are encountered while solving the integral equation governing the surface potential distribution. At certain frequencies the equation fails to yield a unique solution. These frequencies correspond to internal eigenfrequencies (or resonant frequencies) of the geometry under consideration. This nonuniqueness manifests itself when numerically solving the integral equation by causing the coefficient matrix of the system of linear algebraic equations which results from the application of approximate quadrature to the integral equation to become ill-conditioned, causing large numerical errors.

Using a method proposed by Burton and Miller (Ref. 13 of Appendix A), this behavior can be eliminated. This method consists of adding the integral equation for the normal velocity multiplied by a coupling constant. It is then proven that the solution for the acoustic potential field from the combined equation is unique for imaginary values of the coupling constant. This analytical method was therefore incorporated in this study. Although other techniques can be used to avoid the uniqueness problem at certain frequencies (Refs. 4, 6, and 14 of Appendix A), the combined integral equation of Burton and Miller was found to give the best results, and it required minimum computation times.

In order to use the Burton and Miller method two problems had to be resolved. First, a strong singularity exists in the integrand of the combined integral equation developed by Burton and Miller. In the present study, this equation was reformulated to obtain an equation containing only weakly singular terms which could be handled numerically. The second problem is connected with the choice of the coupling constant used by Burton and Miller in combining the integral equations for the potential and normal velocity. It has been found in this study that an optimum value for this parameter for use in numerical computations can be found. Although Burton and Miller showed that the parameter must contain a nonzero imaginary component, they gave no indication of how the results are affected by this parameter. The value which gives the best numerical results is  $i/k$  where  $i = \sqrt{-1}$  and  $k$  is the wave number.

### III. NUMERICAL METHOD

#### A. Integration Procedure

To determine the acoustic field associated with a geometry, the integral equation describing the surface potential distribution must first be solved. Using this distribution, the potential at any exterior point can then be determined to generate the far field sound pattern. For general geometries, the integral equations cannot be solved exactly, and approximate methods must be used. These methods result in a system of linear, algebraic equations with complex coefficients which can be solved by complex Gauss-Jordan reduction to obtain the acoustic potential distribution at the surface.

For the axisymmetric formulation used in this investigation, the surface shape is defined by a line in the radial  $r$  and axial  $z$  directions, and this line is rotated about the axis. The integral equation can then be separated into two line integrals; one in the tangential direction and one along the surface contour in the  $r - z$  plane. In the tangential direction, the line integrals are given by Eqns. (15)-(17) of Appendix B, which, in general, must be solved numerically. A 96-point Gaussian quadrature formula was used to evaluate these integrals. The computational error is approximately inversely proportional to the number of points used to evaluate the integrals in the tangential direction. Along the surface contour in the  $r - z$  plane, the integration of Eq. (18) in Appendix B is required. The integral over the perimeter is first separated into integrals over  $n$  subintervals of either constant or varying lengths. The acoustic potential is assumed constant over each subinterval and it is taken outside the integral. Finally, a two-point Gaussian quadrature formula is used to evaluate the components of the functions defined by Eqs. (15)-(17) of Appendix B in the  $r - z$  plane over each subinterval. Increasing the order of the Gaussian quadrature does not sig-

nificantly affect the accuracy of the computations. However, the error was found to decrease proportionately as the number subintervals  $n$  was increased.

In another solution approach, the potential was assumed to vary linearly over each interval in order to improve the accuracy of the correct potential values. However, the results using this linear interpolation scheme were not as accurate as in the above-mentioned approach. The cause of the inaccuracies in this scheme have not been extensively studied because of time restrictions. However, the errors appear to arise from the implementation procedure used. When linear interpolation was applied to a finite cylinder, problems arose at the corner points. At these points the normal to the surface appearing in the integral equation is undefined. If the potential is assumed constant over each subinterval, subintervals can be taken on either side of this point which in effect avoids the corner points. The method used in applying the linear interpolation about these points strongly influences the computed results. Although several techniques were tried, none proved entirely satisfactory. Also, for general surfaces for which the subintervals may be of unequal length, the difficulty in implementing the linear interpolation technique and its questionable value make this method impractical. Therefore, it will not be used in future studies unless significant improvements can be made.

In another study involving the numerical evaluation of the integral equations, the effect of the coupling constant ( $\alpha$  appearing in Eq. (23) of Appendix A) was investigated. In the method of Burton and Miller, the integral equations for the acoustic potential and normal velocity at the surface are combined into one equation. The terms from the potential equation are of order  $k$  whereas the terms from the expression for the normal velocity are of

order  $k^2$ . Thus, as the frequency is increased, the terms of order  $k^2$  dominate. The results become less accurate because the combined equation in effect becomes the equation for the normal velocity. This equation, like the integral formula for the acoustic potential, yields large errors at certain frequencies when numerically evaluated. By choosing the coupling constant to be  $i/k$ , the terms of order  $k^2$  are now reduced to order  $k$ . Now, as the frequency is increased, the terms from the expression for the normal velocity do not become dominant, and the uniqueness problem is avoided at all frequencies.

#### B. Evaluation of Geometric Parameters and Boundary Conditions

The geometric parameters appearing in the integral Helmholtz equation (see Equation (23) of Appendix A) are the distances between points on the surface, the normal vector at each point, and the lengths of the subintervals in the axial plane. The method for computing these parameters is presented in Section III of Appendix C.

There are two types of boundary conditions which must be specified over the surface. The first consists of a forcing function which generates the acoustic field. In a jet engine inlet, most of the acoustic field is produced by disturbances caused by the interaction between the flow field produced by the fan blades and the stator waves. A literature search was conducted to determine the spatial dependence of the sound generated by the stator-blade interaction so that the resulting radiated sound pattern could be computed. Because of the complexity of the resulting expressions<sup>4</sup>, there was not sufficient time to use these predictions in the present research effort. However, both the analytical and numerical methods used in computing the radiated sound field in the present study are capable of handling forcing functions

of arbitrary spatial dependence in the  $r - z$  plane, such as those encountered in jet engine inlets.

The second type of boundary condition is given by specifying the reaction of the surface to the wave motion. For rigid surfaces, the normal velocity (i.e., the normal derivative of the acoustic potential) is zero and all the sound incident on the surface is reflected. For nonrigid or sound absorbing surfaces, the normal velocity is nonzero since the surface now vibrates in response to the wave motion. The normal velocity at the surface is proportional to the pressure oscillations (i.e., the acoustic potential) of the surrounding fluid and the constant of proportionality is called the surface admittance. The integral wave equation involves both the acoustic potential and the normal acoustic velocity which means there is one equation for two unknowns. By using the admittance relationship, the normal velocity can be expressed in terms of the acoustic potential and the admittance. The resulting equation can then be solved for the potential.

The admittance is a measure of the sound absorption characteristics of the surface. In jet engine inlets the surfaces are often lined with Helmholtz resonator arrays which absorb sound and reduce the noise radiated to the surroundings. Expressions for the admittances of these sound absorbing devices have been derived<sup>5</sup> and they can be used in the present investigation. In fact, the capability exists to predict the sound field produced from a jet engine inlet for arbitrary sound source and admittance characteristics.

### C. Computer Program

A computer program written in Extended FORTRAN IV has been developed for use on a CDC CYBER 70 computer for solving the system of linear algebraic equations which result from the numerical approximation to the integral wave equation. This program has been thoroughly checked out using

simple geometries for which exact solutions can be obtained. The program employs standard functions common to all FORTRAN compilers so that it can be used with minimum modifications on other computers. Generality is maintained in order to accommodate arbitrary surface geometries and boundary conditions. In the cases run to date, the computation time for determining the surface potential is given by the following approximate formula

$$t = 0.05 (n)^2$$

where  $t$  is the computation time in seconds and  $n$  is the number of subintervals used in the numerical evaluation of the integral equation. Approximately one second per point is required for the far field potential. For the cases run thus far, the run times have been from 20 to 140 seconds for 20 to 53 subintervals. Efforts toward maximizing the programming and numerical efficiency have resulted in these relatively short run times.

#### IV. RESULTS AND SUMMARY

##### A. Simple Geometries

To check the numerical schemes used in this investigation, preliminary computations using a sphere and a cylinder of finite length were obtained. The results are presented in Section III of Appendix B. In all cases, 20 subintervals were taken in the  $r-z$  plane and a 20-point Gaussian quadrature was used to evaluate the integrals in the tangential direction. The results for these simple geometries can be summarized as follows:

- (1) The coupling parameter used in the Burton and Miller ( $\alpha$  in Eq. (23) Appendix A) should be taken as  $i/k$  where  $k$  is the wave number and  $i$  is  $\sqrt{-1}$ .

- (2) For the cylinder, the error in the computed results increases with increasing frequency. For continuous boundary conditions the error is less than 10% at all frequencies.
- (3) Discontinuous boundary conditions, where the admittance is specified over part of the surface and a forcing function over the remainder, decrease accuracy of the results. The computed and exact values agree to within 10% for low nondimensional wave numbers (i.e.,  $ka < 5$  where  $a$  is the radius of the cylinder). Errors of 40% at the point of discontinuity occur at a nondimensional wave number of 10. The remainder of the points agree to within 12% at this frequency.
- (4) In the tangential plane, the spatial distribution of the acoustic potential varies as  $\cos m \theta$  where  $m$  is an integer. Increasing  $m$  does not affect the accuracy of the results significantly.
- (5) The computed far field acoustic potentials are at least as accurate as the computed surface potentials.
- (6) The far field results are accurate at distances greater than the length of one subinterval from the surface.

#### B. Inlet Configuration

The studies of the acoustic fields of the sphere and cylinder served to evaluate and refine the numerical procedures and programming techniques. The next configuration investigated was an inlet used in a study by NASA<sup>6</sup>. This inlet is shown in Fig. 1 and it was chosen because:

- (1) unlike most inlets used in research studies, it does not have a bell-mouth shape but is shaped like a typical inlet used in existing aircraft;

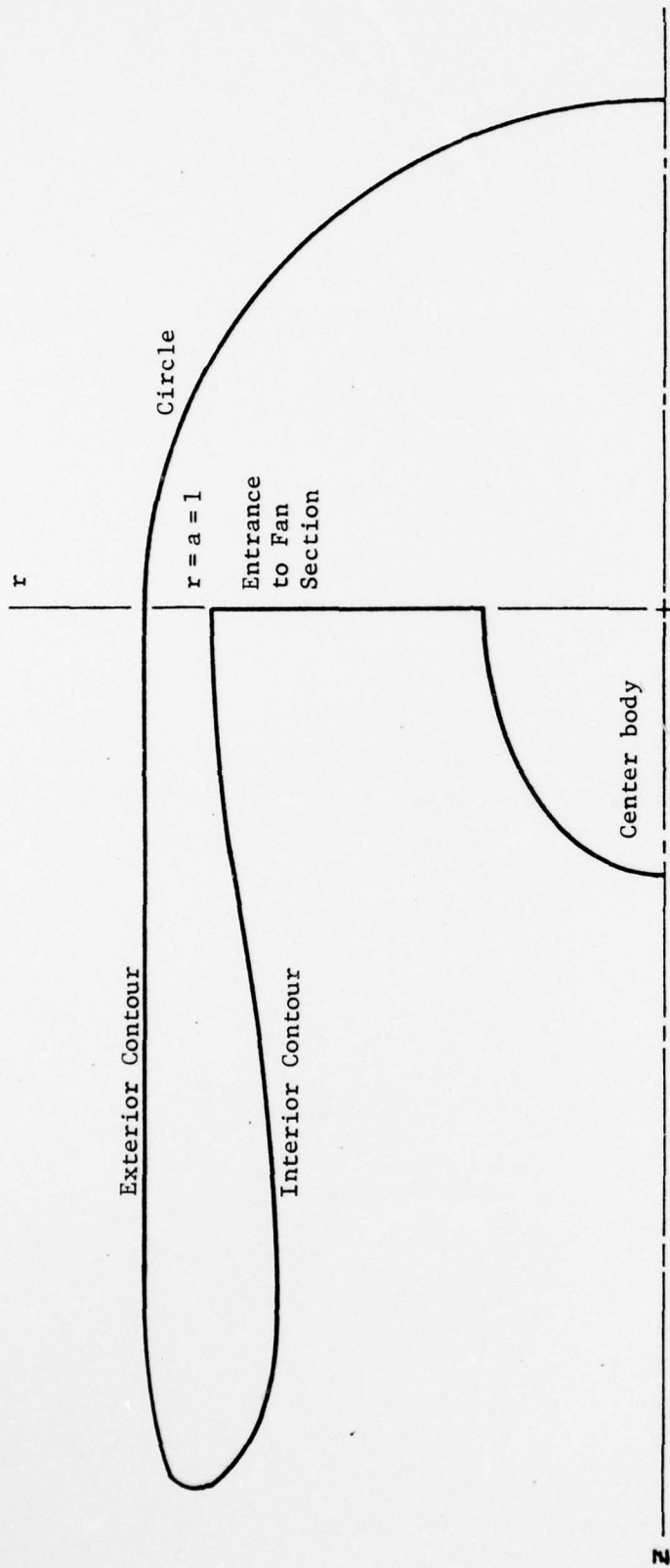


Figure 1. Inlet Geometry

- (2) complete details on generating the inlet boundary are given; and
- (3) it is being used in a related study being conducted at Georgia Tech concerning the prediction of the sound field inside the inlet; so the sound field, at least inside the duct, can be compared with results obtained independently by other numerical methods.

The back side of the inlet is presently assumed to be spherical.

To obtain exact results for comparison with the numerical computations, a spherical source was assumed to be placed at  $(r,z) = (0,0)$ . The acoustic potential and normal velocity for this source can be readily computed at every point. In particular, they can be computed on the surface of the inlet. The value of the normal velocity at each point along the surface of the inlet is then used as the boundary condition in the integral equation. From this boundary condition the value of the potential can then be numerically computed using the techniques described in Chapter III and compared with the exact potential known from the spherical source solution. As seen in Fig. 2, the normal acoustic velocity distribution, which represents a forcing function is highly discontinuous and it provides a severe test of the numerical techniques employed.

The numerical and exact solutions for the surface acoustic potential are compared in Fig. 2 for 32 and 54 subintervals taken along the perimeter of the inlet in the  $r-z$  plane. Because of the errors in approximating the lengths of each subinterval, the exact solutions differ slightly as the distance along the perimeter  $S$  increases. The centerbody in Fig. 1 extends from  $0 \leq S \leq 0.8$ , the fan inlet covers  $0.8 < S \leq 1.4$ , the interior contour extends from  $1.4 < S \leq 3.5$ , the exterior from  $3.5 < S \leq 5.5$ , and the circular arc lies within the interval

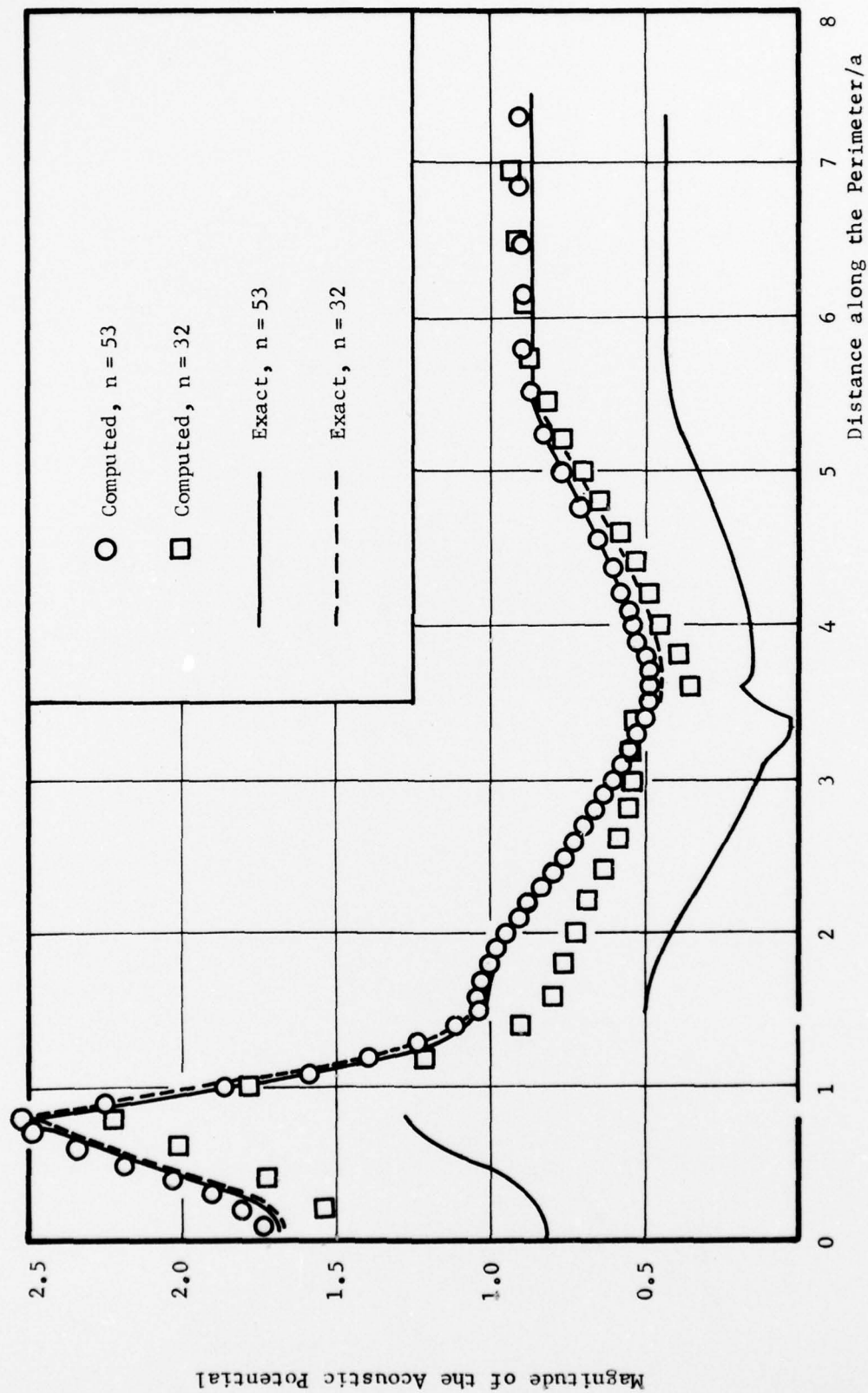


Figure 2. Effect of Increasing the Number of Subintervals in Computing the Surface Potential for the Inlet Configuration at  $k a = 1$ ,  $m = 0$ .

$5.5 < S \leq 7.45$ . Increasing the number of points decreases the error proportionately as indicated by the data in Fig. 2 at a nondimensional frequency to  $a$  of unity, where  $a$  is the radius of the inlet at the fan entrance section. The absolute average error in the results decrease from 10.2 per cent for 32 subintervals to 4.16 per cent for 53 subintervals. The computation time increased from 53 seconds to 143 seconds, respectively.

As shown in Fig. 3, the errors increase with increasing frequency. Like the cylinder, the maximum error of the potential for the inlet configuration occurs at the points of discontinuity. The average error increases from 4.16 per cent at  $ka = 1$  to 15 per cent at  $ka = 10$ .

For the data in Figs. 2 and 3, the acoustic potential is assumed constant in the tangential plane. The results for a  $\cos(m\theta)$  distribution are presented in Fig. 4 at  $ka = 2$ . These results show the insensitivity of the accuracy of the computed results to the tangential distribution for  $m = 1, 2$ .

Based on the results obtained thus far, the numerical and programming techniques are capable of yielding reliable results for arbitrary geometries and boundary conditions. At higher frequencies, ( $ka < 5$ ) it appears that more points must be taken to increase the accuracy of the computed results.

Next year, experiments will be conducted to measure the acoustic field radiated from an open-ended pipe for comparison with the computed results. A parametric study of the effect of the placement and quality of sound treatment on sound abatement in an inlet configuration will be conducted. Further improvements in the programming and numerical methods will also be investigated.

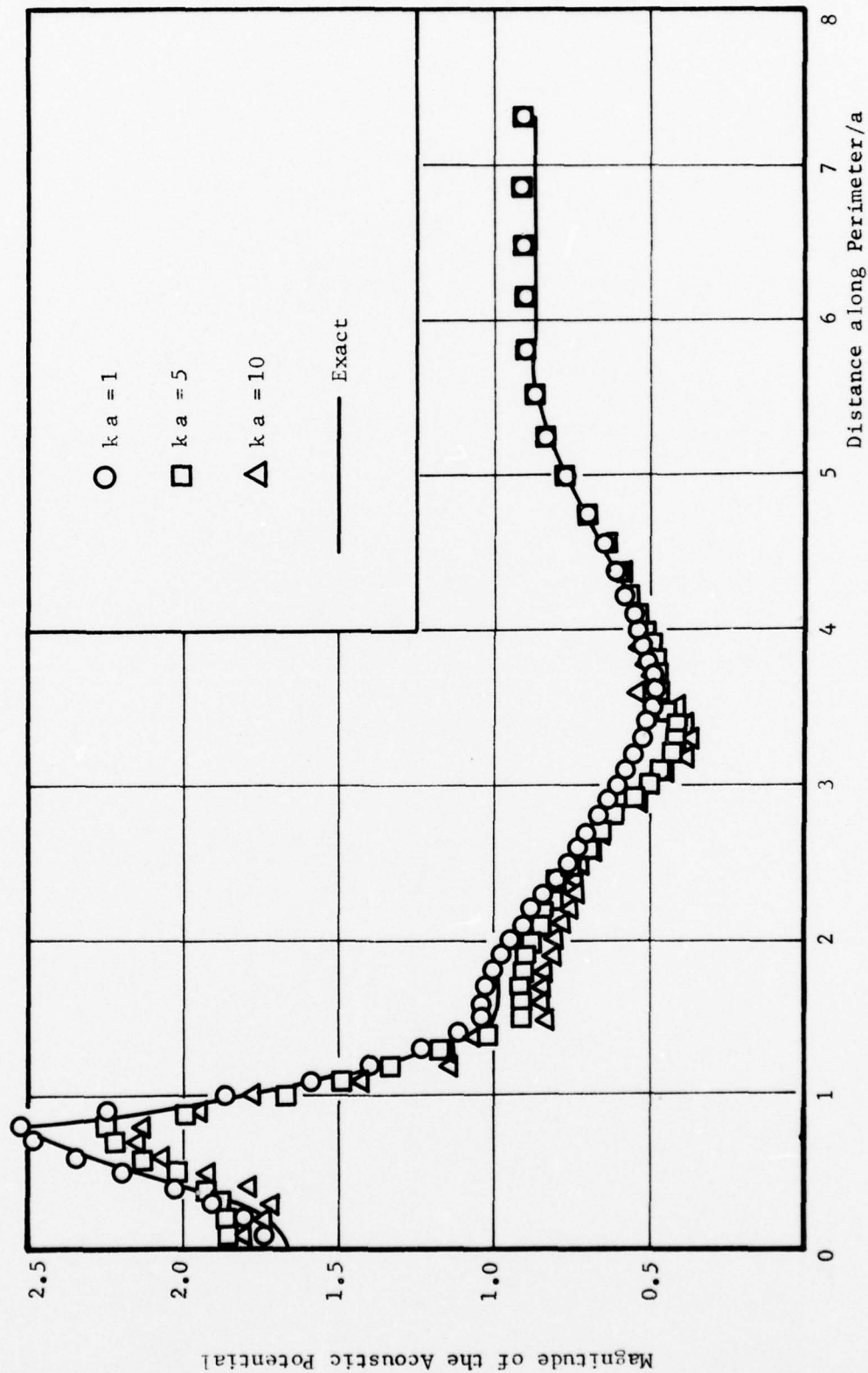


Figure 3. Effect of Increasing Frequency for the Inlet Configuration at  $m = 0$ ,  $n = 53$  on the Computed Surface Potential.

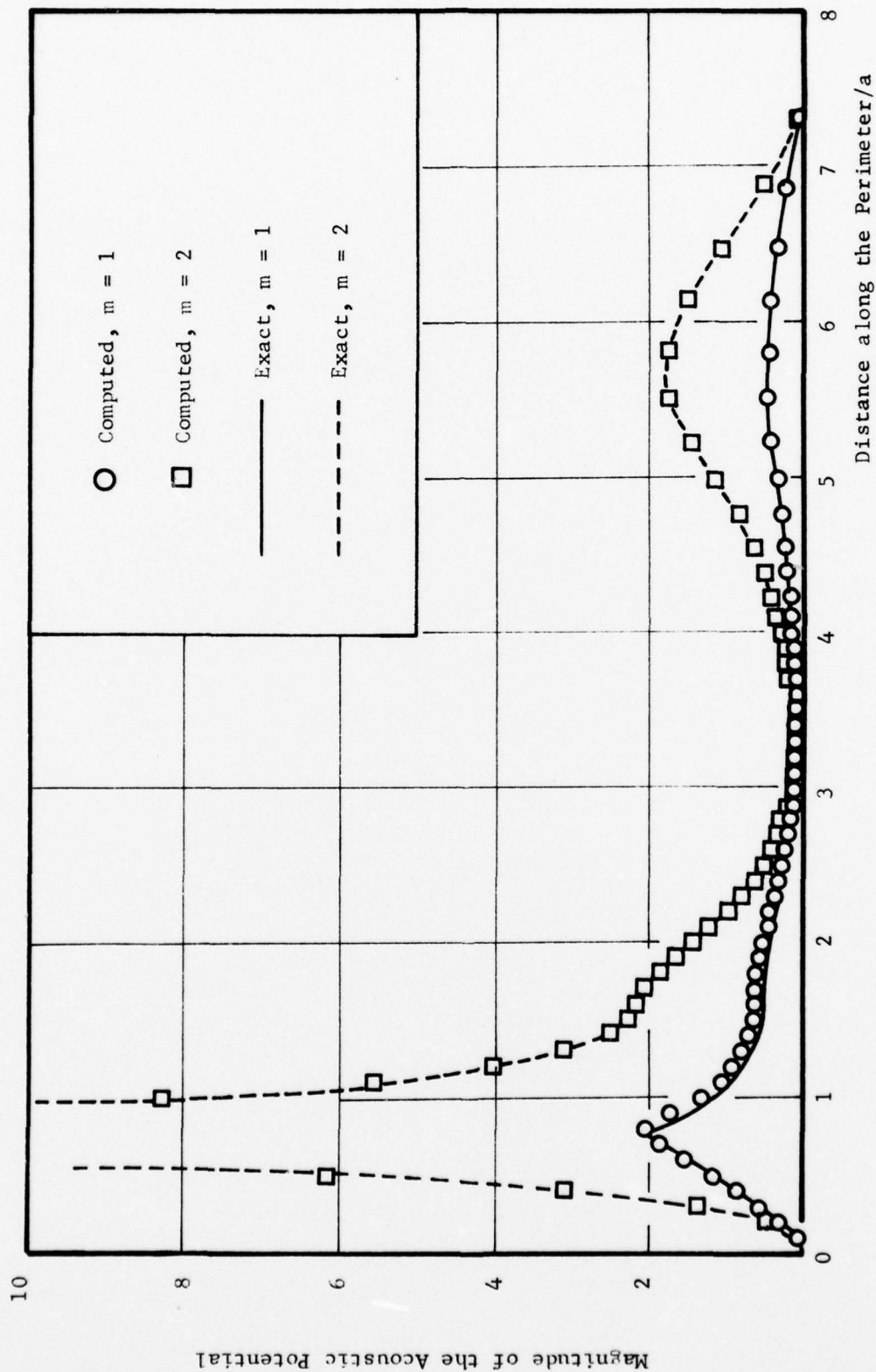


Figure 4. Effect of Mode Number  $m$  on the Computed Surface Potential of the Inlet Configuration for  $ka = 2$  and  $n = 53$ .

#### REFERENCES

1. Meyer, W. L., Bell, W. A., and Zinn, B. T., "Boundary Integral Solutions of Three Dimensional Acoustic Radiation Problems," accepted for publication in the Journal of Sound and Vibration.
2. Meyer, W. L., Bell, W. A., and Zinn, B. T., "Prediction of the Sound Field Radiation from Axisymmetric Surfaces," AIAA Paper No. 78-195, presented at the AIAA 16th Aerospace Sciences Meeting, Huntsville, AL., January 1978.
3. Bell, W. A., Meyer, W. L., and Zinn, B. T., "Predicting the Acoustics of Arbitrarily Shaped Bodies Using an Integral Approach," AIAA Journal, Vol. 15, No. 6, June 1977, pp. 813-820.
4. Goldstein, M. E., Aeroacoustics, McGraw-Hill, 1976, Chapter 4.
5. Bell, W. A., Daniel, B. R., and Zinn, B. T., "Acoustic Liner Performance in the Presence of a Mean Flow and Three-Dimensional Wave Motion," AIAA Paper No. 74-61, presented at the AIAA 12th Aerospace Sciences Meeting, Washington, D. C., January 30 - February 1, 1974.
6. Miller, B. A., Dastoli, B. J., and Wesoky, H. L., "Effect of Entry-Lip Design on Aerodynamics and Acoustics of High-Throat-Mach-Number Inlets for the Quiet, Clean, Short-Haul Experimental Engine," NASA TM- X-3222, May 1975.

APPENDIX A

Integral Solutions of Three Dimensional  
Acoustic Radiation Problems<sup>\*</sup>

W. L. Meyer<sup>\*\*</sup>, W. A. Bell<sup>†</sup>, B. T. Zinn<sup>††</sup>

School of Aerospace Engineering  
Georgia Institute of Technology  
Atlanta, Georgia 30332

---

\* This research was partially supported by AFOSR grant number F49620-77-C-0066.

\*\* Research Associate, † Research Engineer, †† Regents' Professor

### Abstract

This paper is concerned with the development of a procedure for generating the sound fields radiated by arbitrarily shaped, three dimensional bodies from an integral representation of the solutions of the Helmholtz equation. The method of Burton and Miller is employed to eliminate the nonuniqueness in the external Helmholtz formulae which occurs at the internal eigenfrequencies of the geometry under consideration. Also, a representation of the most singular component in the Burton and Miller formulation is developed resulting in an integral equation which is amenable to numerical solutions. A simple numerical scheme is introduced which reduces the large amounts of computer storage and time normally required for the solution of similar problems. This numerical scheme is then used to obtain solutions for the radiated sound field generated by a vibrating piston set in a sphere. The numerical solutions for the surface and far field sound patterns are compared with exact analytical solutions and deviations of ten percent at most are noted. Since the symmetry of the sphere was not taken advantage of in these computations, the numerical schemes employed are applicable to general three dimensional sound radiation problems.

### I. Introduction

The development of a simple analytical form and an efficient numerical method for the prediction of the characteristics of the sound fields radiated by three dimensional bodies is the main concern of this paper. Such prediction techniques have a variety of applications in science and engineering; for example, the determination of the sound fields radiated by aircraft and underwater vehicles. The approach developed in this investigation is by no means limited to acoustic radiation problems as other wave phenomena are governed by similar equations. Thus, the analytical and numerical methods employed here are also directly applicable to other fields of engineering such as electromagnetic antenna theory

and wave scattering problems.

This research was undertaken with the objective of determining the applicability of certain integral equation formulations for the exterior Helmholtz problem in the prediction of the radiated sound fields produced by three dimensional bodies. In principle, integral formulations appear very attractive as they (1) eliminate the need to consider the infinite domains normally associated with radiation problems; (2) reduce the dimensionality of the problem by one (e.g., from a three dimensional partial differential equation to a two dimensional surface integral equation); and (3) can readily handle arbitrary geometries and boundary conditions. All three properties are very advantageous from a computational point of view as the first two significantly reduce the computer storage requirement for solution and the third eliminates the need to extensively modify the computer code when the geometry or the boundary conditions are altered.

Difficulties arise, however, in the use of the Helmholtz formulae as their solution depends upon the numerical evaluation of singular, oscillatory integrands.<sup>1-5</sup> Also, most external boundary integral representations suffer from a nonuniqueness of the solution at frequencies corresponding to the eigenfrequencies of the associated internal problem of the same geometry.<sup>6-8</sup> Keeping these difficulties in mind, the work presented in this paper is specifically concerned with the following problems: (1) the development of an accurate and efficient numerical scheme for handling the oscillatory, singular integrands encountered in the application of the Helmholtz formulae; (2) the determination of the most effective procedure for handling the nonuniqueness of the radiation solution at eigenvalues of the associated internal acoustic problem; and (3) the determination of the accuracy of the resulting solutions.

While there are many papers in the literature (e.g., see Refs. 1-8) dealing with integral solutions of radiation problems, none of these addresses the important problem of determining the applicability and relative efficiency of the various integral formulations and numerical procedures which can be employed to obtain the desired solutions. Instead, most of these investigations are limited to discussions of the potential advantages of the use of certain integral formulations, various possible approaches for the numerical solution of the resulting integral equations, the nonuniqueness of the solutions of the integral equations which govern the radiation problems, and potential means for alleviating this nonuniqueness problem. The few papers (e.g., see Refs. 1-6 and 9) that deal with the numerical solutions of specific problems are either limited to two dimensional problems or three dimensional problems with simple boundary conditions, such as perfectly reflecting surfaces, which greatly simplify the analytical form and the numerical solution procedure. In the present investigation the analytical and numerical schemes are applied to problems involving general boundary conditions.

## II. Theoretical Considerations.

In this section an outline of the development of the theory upon which the calculations are based is presented. The basic integral representation of the solution of the Helmholtz equation is rigorously developed in Ref. (10) and will not be repeated here; however, derivations that are directly related to the present investigation are presented in detail.

### A. Formulation of the Integral Equation

The standard three dimensional Helmholtz formula for an external (radiation) problem is<sup>7,10</sup>

$$\int \int_{S_q} \left\{ \varphi(Q) \frac{\partial G(P,Q)}{\partial n_q} - G(P,Q) \frac{\partial \varphi(Q)}{\partial n_q} \right\} dS_q = 4 \pi \varphi(P)$$

(1)

(See Fig.1.) where  $G(P,Q)$  is a fundamental solution of the Helmholtz equation; that is:

$$G(P,Q) = \frac{e^{ikr(P,Q)}}{r(P,Q)} \quad (2)$$

and  $k$  is the wave number. In Eq. (1)  $\frac{\partial}{\partial n_q}$  represents an outward normal derivative with respect to the body (i.e. inward with respect to the exterior region) of the function with respect to the variable  $Q$ ; i.e.

$$\frac{\partial \varphi(Q)}{\partial n_q} = \vec{\nabla}_q \varphi(Q) \cdot \vec{n}_q \quad (3)$$

where  $\varphi$  is the acoustic potential.

Introducing the modified admittance,  $Y$ , defined as

$$Y(Q) = \frac{\partial \varphi(Q)}{\partial n_q} / \varphi(Q) \quad (4)$$

Eq. (1) can be rewritten as

$$\int \int_{S_q} \varphi(Q) \left\{ \frac{\partial G(P,Q)}{\partial n_q} - G(P,Q) Y(Q) \right\} dS_q = 4\pi \varphi(P) \quad (5)$$

Thus, using Eq. (1) or Eq. (5), the acoustic potential  $\varphi(P)$  at any point outside the surface of the body  $S$  can be determined if the acoustic potential on the surface of the body  $\varphi(Q)$  and either its normal derivative  $\frac{\partial \varphi(Q)}{\partial n_q}$  (the acoustic velocity) or the admittance  $Y(Q)$  on the surface of the body are known.

If the point  $P$  is allowed to approach the surface of the body, Eq. (5) becomes

$$\int \int_{S_q} \left\{ \varphi(Q) \frac{\partial G(P,Q)}{\partial n_q} - G(P,Q) \frac{\partial \varphi(Q)}{\partial n_q} \right\} dS_q = 2\pi \varphi(P) \quad (6)$$

if the surface  $S$  is sufficiently smooth. Using Eq. (4), Eq. (6) becomes

$$\int_{S_q} \varphi(Q) \left\{ \frac{\partial G(P,Q)}{\partial n_q} - G(P,Q) Y(Q) \right\} dS_q = 2\pi\varphi(P) \quad (7)$$

The integral Eqs. (6) or (7)\* can now be solved for the acoustic potential on the surface if either the acoustic velocity or the admittance is known at each point on the body. Also if the acoustic velocity is known over part of the body (i.e. the driving surface) and the admittance over the remainder, Eq. (6) may be applied on the driving surface and Eq. (7) over the rest of the body.

Both  $G$  and its first normal derivative with respect to the variable  $Q$ , which appear in the kernels of Eqs. (6) and (7), become singular when the point  $Q$  approaches the point  $P$  on the surface (See Eq. (2)). It can be shown, however, that the integrals are regular in spite of this singularity of the kernels, and no analytical problems arise because of it. However, the singular kernels do present numerical difficulties which will be discussed in Section III.

An analytical problem does arise in the solution of Eqs. (6) and (7) when the wave number  $k$ , which appears in the simple source solution  $G$  (See Eq. (2).) approaches a resonant frequency (i.e. an eigenvalue) of the related internal problem.<sup>7,11</sup> At these frequencies Eqs. (6) and (7) do not yield a unique solution.

#### B. The Uniqueness Problem

Since the uniqueness problem occurs only at certain wave numbers corresponding to internal eigenvalues it might be suggested that the problem be simply avoided by considering only wave numbers which are not close to internal

---

\* It will be noted here that Eq. (7) yields a homogeneous set of equations if only the admittance is known. Thus to obtain a unique solution the acoustic potential must be known on part of the body.

eigenvalues. This is not feasible, however, because: (1) if the body is truly arbitrary in shape the internal eigenvalues are not known a priori and the corresponding internal problem would also have to be solved in order to determine what wave numbers to avoid; (2) the integral equation is discretized for numerical integration, which results in a system of algebraic equations, so that there is no longer a specific value but a range of values at which the coefficient matrix becomes ill-conditioned which results in large numerical errors;\* and (3) the interval between successive eigenvalues decreases with increasing wave number and it becomes impossible to stay "sufficiently" far away from the internal eigenvalues at high wave numbers (e.g.,  $k$  on the order of 10).

It has been suggested<sup>6</sup> that one method to assure the uniqueness of the solution is to obtain an overdetermined system of algebraic equations by combining the system of algebraic equations generated from the standard integral equation (e.g., Eq. (6)) with additional algebraic equations generated from the integral relation

$$\int \int_{S_q} \left\{ \varphi(Q) \frac{\partial G(P,Q)}{\partial n_q} - G(P,Q) \frac{\partial \varphi(Q)}{\partial n_q} \right\} dS_q = 0 \quad (8)$$

where the point  $P$  lies inside the surface  $S$ . There are two problems with this approach. The first is determining the number of extra relations required to "pick-out" the proper solution from the set of possible solutions of the non-unique integral equation; and, the second is choosing the placement of the

---

\* If the admittance is non-zero the internal eigenvalues of the problem are in general complex. However, even if only real wave numbers are considered the nonuniqueness problem still exists if the imaginary part of the complex eigenvalue is sufficiently close to zero.

points which are used to generate the extra relations. As there is no known procedure for choosing either the optimum number of extra relations or the points from which they are generated, this method can not be relied upon to give consistently good results.

Ursell<sup>12</sup> has suggested that the uniqueness problem be avoided by the use of a different fundamental solution (i.e. a different G function; see Eq. (2)). Although the use of a different fundamental solution does not change the resulting integral equations and analytically eliminates the uniqueness problem rather elegantly, the function itself is difficult to construct numerically as it entails the computation of infinite series. Thus the elegance of the method is offset by the large increases in computer time and storage required for its implementation, especially when considering three dimensional problems.

Another method for overcoming the uniqueness problem is based upon the fact that a unique solution can be obtained by solving a modified integral equation consisting of the original integral equation (6) and its differentiated form<sup>7</sup>, that is

$$\iint_{S_q} \left\{ \varphi(Q) \frac{\partial^2 G(P,Q)}{\partial n_p \partial n_q} - \frac{\partial G(P,Q)}{\partial n_p} \frac{\partial \varphi(Q)}{\partial n_q} \right\} dS_q = 2\pi \frac{\partial \varphi(P)}{\partial n_p} \quad (9)$$

Equation (9) also describes the behavior of the acoustic potential on the surface of the body, and it has a set of related internal eigenvalues which is mutually exclusive of the set of related internal eigenvalues of Eq. (6). Thus, neither equation ever fails to yield a unique solution at the same k value as the other. Using this fact, the following linear combination of Eqs. (6) and (9)

$$\begin{aligned}
& \iint_{S_q} \left\{ \varphi(Q) \frac{\partial G(P,Q)}{\partial n_q} - G(P,Q) \frac{\partial \varphi(Q)}{\partial n_q} \right\} dS_q \\
& + \alpha \iint_{S_q} \left\{ \varphi(Q) \frac{\partial^2 G(P,Q)}{\partial n_p \partial n_q} - \frac{\partial G(P,Q)}{\partial n_p} \frac{\partial \varphi(Q)}{\partial n_q} \right\} dS_q \\
& = 2\pi \left( \varphi(P) + \alpha \frac{\partial \varphi(P)}{\partial n_p} \right)
\end{aligned} \tag{10}$$

where  $\alpha$  is a coupling constant, should yield a unique solution for all values of the wave number  $k$ .

Specifically, Burton and Miller<sup>13</sup>, have shown that the following relationships exist between the coupling constant  $\alpha$  and the wave number  $k$

$$\text{Im}(\alpha) \neq 0 \rightarrow k \text{ real or imaginary}$$

$$\text{Im}(\alpha) = 0 \rightarrow k \text{ complex} \tag{11}$$

which assures a unique solution. Unfortunately, the differentiated form of the integral equation (9) contains the following term

$$\iint_{S_q} \varphi(Q) \frac{\partial^2 G(P,Q)}{\partial n_p \partial n_q} dS_q \tag{12}$$

which is strongly singular as the point  $Q$  approaches the point  $P$ . Because of its singular form this term cannot be directly integrated numerically.

Two methods for approaching this problem have been suggested. The first solution is to "regularize" the singular component by an integration of the entire equation<sup>14</sup> (See Eq. (10).). This method requires an excessive amount of computing time as an additional integration must be performed over the surface of the body. The other approach suggests the use of a transformation to interpret the singular integral<sup>15</sup> (See Eq. (12).). In Ref. (15) two alternate

forms of the singular integral are put forth. The first requires further manipulation to be of use as it contains yet another singular integral. The second requires an excessive amount of computer storage space as it necessitates additional information that will allow the computation of the tangential derivative of the acoustic potential on the two dimensional surface of the body. It must also be noted that the acoustic potential is the unknown in most problems so that some differencing procedure is required to generate the solution  $\varphi(Q)$ .

### C. Treatment of the Singular Integral

In this section the first relationship developed in Ref. (15) (See pp. 1283-1284.) is used as a starting point for deriving the desired expressions. It is shown in Ref. (15) that

$$\begin{aligned}
 & \int \int_{S_q} \varphi(Q) \frac{\partial^2 G(P,Q)}{\partial n_p \partial n_q} dS_q \\
 &= \int \int_{S_q} \varphi(Q) (n_p \cdot n_q) \nabla_p \cdot \nabla_q G(P,Q) dS_q \\
 &+ \int \int_{S_q} \varphi(Q) (n_p \times n_q) \cdot (\nabla_p \times \nabla_q G(P,Q)) dS_q \\
 &- \int \int_{S_q} \varphi(Q) n_q \cdot \nabla_q \times (n_p \times \nabla_p G(P,Q)) dS_q
 \end{aligned} \tag{13}$$

The first two integrals on the right hand side are regular; however, the third is not. It is also shown that after some manipulation an alternate form of the third term is

$$\int \int_{S_q} \left[ n_q \times \nabla_q \varphi(Q) \right] \cdot \left[ n_p \times \nabla_p G(P,Q) \right] dS_q \tag{14}$$

This integral is regular so that the singular integral has been shown to be equivalent to the sum of three regular integrals. It should be noted that the first term in this integral,  $[\mathbf{n}_q \times \nabla_q \varphi(Q)]$ , is the tangential derivative of the acoustic potential on the surface of the body alluded to in the previous subsection.

An interesting property of this integral, Eq. (14), is that if the acoustic potential  $\varphi(Q)$  is a constant on the surface of the body, the integral is zero as in this case  $\mathbf{n}_q \times \nabla_q \varphi(Q) = 0$ . Since the two formulations are equivalent it follows that

$$\begin{aligned} & - \int \int_{S_q} \varphi(Q) \mathbf{n}_q \cdot \nabla_q \times (\mathbf{n}_p \times \nabla_p G(P, Q)) dS_q \\ & = \int \int_{S_q} [\mathbf{n}_q \times \nabla_q \varphi(Q)] \cdot [\mathbf{n}_p \times \nabla_p G(P, Q)] dS_q \end{aligned} \quad (15)$$

Writing the third integral on the right hand side of Eq. (13) as

$$\begin{aligned} & - \int \int_{S_q} (\varphi(Q) - \varphi(P)) \mathbf{n}_q \cdot \nabla_q \times (\mathbf{n}_p \times \nabla_p G(P, Q)) dS_q \\ & - \varphi(P) \int \int_{S_q} \mathbf{n}_q \cdot \nabla_q \times (\mathbf{n}_p \times \nabla_p G(P, Q)) dS_q \end{aligned} \quad (16)$$

where  $\varphi(P)$  is a constant with respect to the variable  $Q$ , we see that the last integral is identically zero by setting  $\varphi(Q) \equiv 1$  in Eq. (15).

Hence, the first term in Eq. (16) is not only regular but it can also be readily integrated numerically. As point  $Q$  approaches point  $P$  the entire integral goes to zero. Thus it has been shown that the singular integral which appears in the "unique" formulation of this problem can be expressed in the

following form

$$\begin{aligned}
 & \int \int_{S_q} \varphi(Q) \frac{\partial^2 G(P,Q)}{\partial n_p \partial n_q} dS_q \\
 &= \int \int_{S_q} \varphi(Q) (n_p \cdot n_q) \nabla_p \cdot \nabla_q G(P,Q) dS_q \\
 &+ \int \int_{S_q} \varphi(Q) (n_p \times n_q) \cdot (\nabla_p \times \nabla_q G(P,Q)) dS_q \\
 &- \int \int_{S_q} [\varphi(Q) - \varphi(P)] n_q \cdot \nabla_q \times (n_p \times \nabla_p G(P,Q)) dS_q
 \end{aligned} \tag{17}$$

which will be used in the numerical computations of this paper.

#### D. Computational Considerations

Because of the special form of the fundamental solution of the Helmholtz equation,  $G(P,Q) = G(Q,P)$ , (See Eq. (2).) certain simplifications can be made; specifically

$$\begin{aligned}
 \nabla_p \cdot \nabla_q G(P,Q) &= -\nabla_q^2 G(P,Q) = k^2 G(P,Q) \\
 \nabla_p \times \nabla_q G(P,Q) &= -\nabla_q \times \nabla_q G(P,Q) = 0
 \end{aligned} \tag{18}$$

Using the above relationships Eq. (17) can be rewritten as follows:

$$\begin{aligned}
 & \int \int_{S_q} \varphi(Q) \frac{\partial^2 G(P,Q)}{\partial n_p \partial n_q} dS_q \\
 &= - \int \int_{S_q} \varphi(Q) (n_p \cdot n_q) (ik)^2 G(P,Q) dS_q \\
 &- \int \int_{S_q} [\varphi(Q) - \varphi(P)] n_q \cdot \nabla_q \times (n_p \times \nabla_p G(P,Q)) dS_q
 \end{aligned} \tag{19}$$

To reduce Eq. (19) to a form more amenable to numerical computation it is convenient to let  $\varphi(Q) = 1$  so that

$$\begin{aligned} \int \int_{S_q} \frac{\partial^2 G(P,Q)}{\partial n_p \partial n_q} dS_q \\ = - \int \int_{S_q} (n_p \cdot n_q) (ik)^2 G(P,Q) dS_q \end{aligned} \quad (20)$$

Using Eq. (20) the left hand side of Eq. (19) can be rewritten as

$$\begin{aligned} \int \int_{S_q} \varphi(Q) \frac{\partial^2 G(P,Q)}{\partial n_p \partial n_q} dS_q \\ = \int \int_{S_q} [\varphi(Q) - \varphi(P)] \frac{\partial^2 G(P,Q)}{\partial n_p \partial n_q} dS_q \\ - \varphi(P) \int \int_{S_q} (n_p \cdot n_q) (ik)^2 G(P,Q) dS_q \end{aligned} \quad (21)$$

If Eq. (2) is employed and the indicated differentiations are performed the right hand side, Eq. (21) can be rewritten in the following form

$$\begin{aligned} \int \int_{S_q} [\varphi(Q) - \varphi(P)] \frac{e^{ikr(P,Q)}}{r(P,Q)} \left\{ \left[ (ik)^2 - \frac{3}{r(P,Q)} \frac{ik}{r(P,Q)} + \frac{3}{[r(P,Q)]^2} \right] \right. \\ \left. \frac{\partial r(P,Q)}{\partial n_p} \frac{\partial r(P,Q)}{\partial n_q} - \frac{n_p \cdot n_q}{r(P,Q)} \left[ ik - \frac{1}{r(P,Q)} \right] \right\} dS_q \\ - \varphi(P) \int \int_{S_q} \frac{e^{ikr(P,Q)}}{r(P,Q)} (ik)^2 (n_p \cdot n_q) dS_q \end{aligned} \quad (22)$$

where  $\frac{\partial r(P,Q)}{\partial n_p} = \vec{\nabla}_p r(P,Q) \cdot \vec{n}_p$ . Using the results developed in this section

the formulation of Burton and Miller<sup>13</sup> (See Eq. (10).) reduces to

$$\begin{aligned}
 & \int \int_{S_q} \varphi(Q) \frac{e^{ikr(P,Q)}}{r(P,Q)} \left( ik - \frac{1}{r(P,Q)} \right) \frac{\partial r(P,Q)}{\partial n_q} dS_q \\
 & - \alpha \varphi(P) \int \int_{S_q} \frac{e^{ikr(P,Q)}}{r(P,Q)} (ik)^2 (n_p \cdot n_q) dS_q \\
 & + \alpha \int \int_{S_q} [\varphi(Q) - \varphi(P)] \frac{e^{ikr(P,Q)}}{r(P,Q)} \left\{ \left[ (ik)^2 - \frac{3ik}{r(P,Q)} + \frac{3}{[r(P,Q)]^2} \right] \right. \\
 & \quad \left. \frac{\partial r(P,Q)}{\partial n_p} \frac{\partial r(P,Q)}{\partial n_q} - \frac{n_p \cdot n_q}{r(P,Q)} \left( ik - \frac{1}{r(P,Q)} \right) \right\} dS_q \\
 & - \int \int_{S_q} \frac{\partial \varphi(Q)}{\partial n_q} \frac{e^{ikr(P,Q)}}{r(P,Q)} dS_q \\
 & - \alpha \int \int_{S_q} \frac{\partial \varphi(Q)}{\partial n_q} \frac{e^{ikr(P,Q)}}{r(P,Q)} \left( ik - \frac{1}{r(P,Q)} \right) \frac{\partial r(P,Q)}{\partial n_p} dS_q \\
 & = 2 \pi (\varphi(P) + \alpha \frac{\partial \varphi(P)}{\partial n_p})
 \end{aligned} \tag{23}$$

The above equation, although it may appear more complicated, is actually considerably simpler from a numerical point of view than solving Eq. (10) with Eqs. (13) and (14). In summary, the above formulation of the sound radiation problem provides unique solutions at all wave numbers  $k$  and contains no singular integrals.

### III. Numerical Considerations.

To determine the radiated sound field generated by an arbitrarily shaped three dimensional body, Eq. (23) must first be solved for the distribution of the acoustic potential on the surface of the body,  $\varphi(Q)$ . Then this data needs

to be substituted into Eq. (1) to determine the radiated sound field. Inspection of Eq. (23) indicates that all of the integrands appearing in this equation are both oscillatory and singular due to the factor  $\frac{e^{ikr(P,Q)}}{r(P,Q)}$  which appears in each. Therefore care must be exercised in the numerical representation of these kernels.

When considering the numerical evaluation of an integral on an arbitrary two dimensional surface, such elegant computational methods as Gaussian quadrature<sup>16,17</sup> (which has been found by the authors of this paper to yield accurate results in two dimensional sound radiation problems<sup>18</sup>) cannot be used in the numerical representation of the kernels. The only simple approach available to obtain a more accurate representation of the kernels is to evaluate them at more points on the surface of the body. Unfortunately, this is usually accompanied by an attendant increase in the size of the coefficient matrix which must be solved to obtain the acoustic potential. The computer time required to solve this matrix goes up roughly as the square of the number of unknowns for most methods of solution (e.g., Gauss-Jordan reduction).

Two considerations enter into the determination of the size of the coefficient matrix: (1) the heuristic determination of the number of points required on the surface of the body to represent the acoustic potential to the desired accuracy; and (2) the computer time and storage space available to solve the coefficient matrix resulting from the discretization of the integral equation. The storage space available is usually much smaller than the number of points required for the accurate evaluation of the singular, oscillatory kernels.

In view of the above considerations the following scheme is used to obtain a numerical solution. First, the surface of the body is divided into a number of area elements which corresponds to the number of points where the acoustic potential is to be calculated on the surface. It has been determined that better results are obtained in general if the area elements are "regular" (i.e.,

not too elongated in any direction), although the exact shape is unimportant, and they should be of roughly equal area. A point is then chosen in the "center" of each area element (usually the centroid of the plane figure projected to the body surface). These points will be denoted as calculational points (i.e. P points) as this is where the acoustic potential will be calculated. Next, each of the original area elements is subdivided into a number of smaller area elements, the sum of which corresponds to the number of points where the singular, oscillatory kernels must be evaluated on the surface of the body to assure their accurate representation. A point is thus chosen on the surface of the body in the "center" of each of the smaller area elements as before. These points will be denoted as computational points (i.e. Q points) since the kernel functions are computed there.

The calculational points may or may not be a subset of the computational points on the surface of the body. If they are a subset some computer space may be saved; however, the computational point must be avoided when it corresponds to a calculational point (i.e. when the point Q corresponds to the point P) since the kernels are then singular. Thus each term in the coefficient matrix is now the sum of a number of terms generated by a number of evaluations of each kernel function.

Since the integrals are all regular a better approximation may be obtained by placing computational points closer to the calculational point when one is close to the singularity of the kernel function. Thus the computational area elements may be further subdivided to obtain a more accurate representation of the integral about the point P.

An illustration of how the above procedure is accomplished is presented below using Eq. (23) which is rewritten in the following more compact form

$$\begin{aligned}
& \int_{S_q} \varphi(Q) A(P, Q) dS_q + \varphi(P) \int_{S_q} B(P, Q) dS_q \\
& + \int_{S_q} [\varphi(Q) - \varphi(P)] C(P, Q) dS_q - 2 \pi \varphi(P) \\
& = 2 \pi \alpha \frac{\partial \varphi(P)}{\partial n_p} + \int_{S_q} D(P, Q) dS_q
\end{aligned} \tag{24}$$

where the proper form of the integrands can be readily obtained. Next, Eq. (24) is discretized as follows:

$$\begin{aligned}
& \sum_{\substack{Q=1 \\ Q \neq P}}^n \varphi(Q) A(P, Q) \Delta S_Q + \varphi(P) \sum_{\substack{Q=1 \\ Q \neq P}}^n B(P, Q) \Delta S_Q \\
& + \sum_{\substack{Q=1 \\ Q \neq P}}^n [\varphi(Q) - \varphi(P)] C(P, Q) \Delta S_Q \\
& + \varphi(P) \sum_{q=1}^m [A(P, q) + B(P, q)] \Delta S_q - 2 \pi \varphi(P) \\
& = \sum_{\substack{Q=1 \\ Q \neq P}}^n D(P, Q) \Delta S_Q + \sum_{q=1}^m D(P, q) \Delta S_q + 2 \pi \alpha \frac{\partial \varphi(P)}{\partial n_p}
\end{aligned} \tag{25}$$

$$P = 1, 2, \dots, N$$

where  $N$  is the number of calculational points;  $n$  is the number of computational points (not including the subdivided element about  $P$ ), and  $m$  is the number of computational points in the subdivided element. In the above representation the normal component of the acoustic velocity,  $\frac{\partial \varphi(Q)}{\partial n_q}$ , on the body is assumed known and is therefore included in the integrand  $D(P, Q)$ . Additional input data required to obtain a solution include: (1) the coordinates of each computational point;

(2) the area associated with each computational point and (3) the outward normal vector at each computational point. The information required at the calculational points is included in the above.

If the resulting matrix of coefficients is large, there are many iterative schemes which can be employed in its solution<sup>19</sup>; however, if the matrix is small Gaussian elimination with back substitution may be used. Once the acoustic potential is determined on the surface, Eq. (1) may be used to generate the acoustic potential at any point in the field surrounding the body. In this computation the point Q never coincides with point P and the integrands are never singular; however, they are still oscillatory and care must still be taken to get an accurate representation of the integrals.

Due to the availability of analytical solutions for comparison purposes, the developed numerical procedure has been applied to predict the sound radiated by a sphere. However, it should be reiterated that no advantage was taken of the sphere's relatively simple geometry (i.e. its symmetry) in the numerical computations. Once the needed input data was generated it was treated like any other arbitrarily shaped three dimensional body. The sphere was subdivided into 80 triangles by first taking an icosahedron (a three dimensional figure whose surface consists of 20 equilateral triangles) inscribed in a unit sphere and dividing each triangle into four others (See Ref. (1), pp. 1630-1631.). This was accomplished by finding the midpoint of each side of each triangle and projecting it to the surface of the sphere as shown in Fig. 2. The centroid of each triangle was then found and also projected to the surface of the sphere. These 80 points correspond to the previously described calculational points.

To obtain the computational points this method was simply repeated three more times yielding 5120 points. Around each calculational point the three surrounding triangles were then divided once more, and at the calculational point

itself the triangle was divided twice more as shown in Fig. 3. The spherical area was then computed for each computational triangle (i.e. the sum of the areas of all the computational triangles is  $4\pi$ , the surface area of the unit sphere). This yielded all the geometrical input data required, as; for a unit sphere the coordinates of the computational points and the elements of the outward normals are the same in rectangular coordinates.

#### IV. Results and Discussion.

In the calculations performed in this study the surface of the radiating sphere was divided into two parts. On one part (the driving surface) the normal acoustic velocity,  $\frac{\partial \varphi}{\partial n}$ , was specified while on the other part (the admittance surface) the modified admittance function  $Y$ , defined by Eq. (4), was specified indicating either sound absorption or amplification by this part of the surface (See Fig. 4.). The sphere was chosen for this study as exact analytical solutions can be obtained for comparison with the numerical solutions obtained by solving the integral equations.

Using the well known separation of variables technique it can be shown that the acoustic potential for the sphere can be represented as follows

$$\varphi(r, \theta, \xi) = h_m(\zeta) \left\{ (1-\eta^2)^{\frac{1}{2}n} \frac{d^n}{d\eta^n} P_m(\eta) \right\} \begin{Bmatrix} \cos n \xi \\ \sin n \xi \end{Bmatrix} \quad (26)$$

either on or in the field surrounding the surface of the sphere. In the above expression  $\eta = \cos \theta$ ,  $\zeta = kr$ ,  $h_m$  is a spherical Hankel function of order  $m$ , and  $P_m$  is a Legendre polynomial of degree  $m$ . It should be noted that when  $n = 0$  all  $\xi$  dependence drops out so that the problem becomes axi-symmetric.

It can also be shown<sup>20</sup> that the acoustic potential for a piston vibrating in an otherwise hard (i.e.  $Y = 0$ ) sphere is given by

$$\varphi(r, \theta, \xi) = \left( \frac{\partial \varphi}{\partial n} / 2k \right) \sum_{m=0}^{\infty} \left[ P_{m-1}(\eta_0) - P_{m+1}(\eta_0) \right] \left\{ \frac{h_m(\zeta)}{\frac{d}{d\zeta} h_m(\zeta_0)} \right\} P_m(\eta) \quad (27)$$

both on the surface of the sphere and in the field surrounding it. In Eq. (27),  $\theta_0$  denotes the edge of the piston set in the sphere,  $a$  is the radius of the sphere,  $\zeta_0 = ka$ ,  $\eta_0 = \cos \theta_0$ ,  $P_{-1}(\eta_0) = 1$  (when  $m = 0$ ), and the remaining quantities are the same as those appearing in Eq. (26). The solution is always axi-symmetric as there is no  $\xi$  dependence. Also, both solutions (i.e., Eqs. (26) and (27)) represent radiated sound fields as they satisfy the necessary radiation conditions when  $r \rightarrow \infty$ .

In all the calculations performed in this study the acoustic velocity is specified on a quarter of the sphere's surface as shown in Fig. 4. Also, the sphere is of unit radius (i.e.  $a = 1$ ) and the coupling constant  $\alpha$ , required in applying the method of Burton and Miller, has been taken as the pure imaginary number  $i$  as  $k$  is a real number (See Eq. (11)).

The radiative fields computed in this study are summarized in Table I where the assigned values of  $m$  and  $n$  describe a specific solution (See Eq. (26)). For each investigated case Table I contains the exact solutions on the surface and far fields, the input boundary conditions derived from the known exact solution, and the average percent error obtained by comparing the exact and computed solutions.

To check the numerical approach and computer code Case # 1 was investigated initially (See Table I.). Under these conditions the analytical solution for the surface potential,  $\phi = h_0(kr)$ , is a constant as is the input data (i.e.  $\frac{\partial \phi}{\partial n}$  and  $Y$ ). A comparison between the numerical and exact solutions for the amplitude  $|\phi|$  of the acoustic potential\* on the surface of the sphere and in the far field is presented in Fig. (5) where excellent agreement between the two solutions is noted. The computation of the surface solution required three minutes of computing

---

\* The amplitude was chosen for comparison as both the real and imaginary parts of the acoustic potential show similar trends and errors.

time on the Georgia Tech CDC Cyber 70 model 74 computer. This time is indicative of all the cases considered in this study. The far field distribution of the acoustic potential was calculated using both the exact surface distribution and the calculated surface distribution. The far field calculation using the exact surface distribution was done as a check on the computer code and the results agreed with the exact solution (obtained from Eq. (26)) to seven significant figures in both the real and imaginary parts. To calculate both distributions simultaneously, under two minutes of computing time was required which is also indicative of all the cases run.

The second investigated solution (See Case # 2, Table I.) was the same solution as Case # 1 but with a wave number  $k = \pi$  which coincides with the first internal eigenvalue of the sphere. This case was run to check the validity of the theory. Again the solution for the surface potential and the input data are constants both on and off the surface of the sphere. A comparison between the computed and exact solutions on the sphere surface and in the far field are presented in Fig. (6). Examination of this figure indicates that in this case the agreement is not as good as in Case # 1, although the average error was still under ten percent. The far field distribution of the acoustic potential was calculated as before. Employing the exact surface distribution the results compared with the exact far field solution to four significant figures in both the real and imaginary parts. In examining Fig. 6 it is interesting to note that there was no increase in the error from the surface distribution to the far field. It was found that there was no significant increase in error from the surface to the far field distribution in any of the cases run.

The exact solution for Case # 3 (obtained from Eq. (26) with the data in Table I) is  $\varphi = h_1(kr) \cos \theta$ . In contrast to the previous cases this solution is  $\theta$  dependent. A comparison between the exact and numerical solutions on the surface of the sphere is presented in Fig. 7, and a far field comparison is pre-

sented in Fig. 8. Examination of the data shows that in this case the error was actually reduced in going from the surface to the far field. Furthermore in the far field, the calculated surface distribution gives better results than does the exact surface distribution.

The next case investigated (Case # 4) was run at the second internal eigenvalue of the sphere,  $k = 4.49340946$ . The results for the acoustic potential on the surface of the sphere are presented in Fig. 9. As can be seen the results deteriorate somewhat at an internal eigenvalue of the problem. It is interesting to note that the error increases with  $\theta$  and it reaches its maximum value at  $\theta = 180^\circ$ , the center of the admittance surface. The results for the far field are presented in Fig. 10. All of the cases considered so far were axisymmetric, that is, there was no  $\xi$  dependence; a property that was also retained by the developed numerical solutions.

This next case (Case # 5) is truly three dimensional as there is a  $\xi$  dependence in the solutions. Referring to Eq. (26) and Table I the exact solution on the surface of the sphere is found to be  $\varphi = h_1(kr) \sin \theta \sin \xi$ . The average percent error was not calculated in this case due to the zeros which appear in the exact solution, but the errors remained small (i.e. under ten percent). The far field distribution of the acoustic potential was calculated and no increase in error was detected.

In the next three cases a hard sphere (i.e.  $Y = 0$  on the admittance surface) with a unit driver (i.e.  $\frac{\partial \varphi}{\partial n} = 1$  on the driving surface) was considered. The exact solutions for these cases can be obtained from Eq. (27). In these studies the wave number  $k$  was varied to determine the value of  $k$  at which the accuracy of the solution deteriorates for a fixed number of 80 calculational points that was used in these numerical studies.

The solution for Case # 6 where  $k = 2$ , are presented in Fig. 11 for both the surface distribution of  $|\varphi|$  and the far field solution. In this case the far field is considered to be at  $kr = 100$ .

In this next case (Case # 7) the wave number is increased to  $k = 5$ . As can be seen from Fig. 12, the error is still under ten percent on both the surface of the sphere and in the far field (i.e.  $kr = 100$ ). When the wave number is increased to  $k = 10$  (Case # 8) the error becomes rather large. The average error in the calculation of the surface potential is sixty percent. So it can be seen that there are not enough calculated points to accurately represent the potential function,  $\varphi$ . The far field is calculated at  $kr = 100$  and the error drops a bit but it still remains high at twelve percent.

#### V. Summary.

In summary, a solution approach has been developed in this paper which may be used to yield a unique solution for the distribution of the acoustic potential on the surface of an arbitrary three dimensional body at all values of the wave number. Also, a numerical scheme was developed to solve the equation accurately and efficiently. Computer programs were run to verify the applicability of the developed solution method and to find its limit of accuracy for a fixed number of points. The procedure was found to be both accurate and versatile as the computer code required no major modifications to handle the various boundary conditions imposed on the surface of the body.

#### Acknowledgement

The authors would like to thank Prof. M. P. Stallybrass for the many helpful discussions concerning some of the theoretical aspects of this paper and Lt. Col. Lowell Ormand, Grant Monitor for his support.

### References

1. Chen, L. H. and Schweikert, D. G., Oct. 1963, Journal of the Acoustical Society of America, Vol. 35, No. 10, pp. 1626-1632, "Sound Radiation From an Arbitrary Body".
2. Banaugh, R. P. and Goldsmith, W., Oct. 1963, Journal of the Acoustical Society of America, Vol. 35, No. 10, pp. 1590-1601, "Diffraction of Steady Acoustic Waves by Surfaces of Arbitrary Shape".
3. Chertock, G., July 1964, Journal of the Acoustical Society of America, Vol. 36, No. 7, pp. 1305-1313, "Sound from Vibrating Surfaces".
4. Greenspan, D. and Werner, P., 1966, Archives of Rational Mechanics and Analysis, Vol. 23, Pt. 4, pp. 288-316, "A Numerical Method for the Exterior Dirichlet Problem for the Reduced Wave Equation".
5. Copley, L. G., Apr. 1967, Journal of the Acoustical Society of America, Vol. 4, No. 4, pp. 807-816, "Integral Equation Method for Radiation from Vibrating Bodies".
6. Schenck, H. A., Jan. 1968, Journal of the Acoustical Society of America, Vol. 44, No. 1, pp. 41-58, "Improved Integral Formulation for Radiation Problems".
7. Burton, A. J., Jan. 1973, NPL Report NAC 30, National Physical Laboratory, Teddington Middlesex, "The Solution of Helmholtz' Equation in Exterior Domains using Integral Equations".
8. Jones, D. S., 1974, Quarterly Journal of Mechanics and Applied Mathematics, Vol. 27, Pt. 1, pp. 129-142, "Integral Equations for the Exterior Acoustic Problem".
9. George, R. C. Tai and Richard P. Shaw, Sept. 1974, Journal of the Acoustical Society of America, Vol. 56, No. 3, pp. 796-804, "Helmholtz- Equation Eigenvalues and Eigenmodes for Arbitrary Domains".

10. Baker, B. B. and Copson, E. T., 1950, The Mathematical Theory of Huygens' Principle, Ch. I, Oxford at the Clarendon Press.
11. Jones, D. S., July 1974, Proceedings of the IEEE, Vol. 121, No. 7, pp. 573-582, "Numerical Methods for Antenna Problems".
12. Ursell, F., 1973, Proceedings of the Cambridge Philosophical Society, Vol. 74, pp. 117-125, "On the Exterior Problems of Acoustics".
13. Burton, A. J. and Miller, G. F., 1971, Proceedings of the Royal Society of London, A323, pp. 201-210, "The Application of Integral Equation Methods to the Numerical Solution of Some Exterior Boundary Value Problems".
14. Panich, O. I., 1965, USP. MAT. NAUK., 20, Pt. 1, pp. 221-226, "On the Question of the Solubility of the Exterior Boundary Problem for the Wave Equation and Maxwell's Equation," (Russian).
15. Stallybrass, M. P., May 1967, Journal of Mathematics and Mechanics, Vol. 16, No. 11, pp. 1247-1286, "On a Pointwise Variational Principle for the Approximate Solution of Linear Boundary Value Problems".
16. Abramowitz, M. and Stegun, I. A., Eds., May 1968, Handbook of Mathematical Functions, Ch. 25, Dover Publications, Inc., New York (5th Printing)
17. Scheid, F., 1968, Theory and Problems of Numerical Analysis, Ch. 15, McGraw-Hill Book Co., New York.
18. Bell, W. A., Meyer, W. L. and Zinn, B. T., July 20-23, 1976, 3rd AIAA Aero-Acoustics Conference, Palo Alto, Calif., AIAA Paper No. 76-494, "Predicting the Acoustical Properties of Arbitrarily Shaped Bodies by Use of an Integral Approach".
19. Isaacson, E. and Keller, H. B., 1966, Analysis of Numerical Methods, Ch. 2, John Wiley & Sons, Inc., New York.
20. Morse, P. M. and Ingard, K. U., 1968, Theoretical Acoustics, p. 343, McGraw-Hill, Inc., New York.

Case #	m	n	k	kr Far Field	Exact Solutions Surface $\varphi =$	Far Field $\varphi =$	Input Conditions Driving Surface $\frac{\partial \varphi}{\partial n} =$ Admittance Surface $Y =$	Average Error %
1	0	0	1	50	$0.841 - 0.540i$	$-0.00524 - 0.0193i$	$-0.301 + 1.38i$ $-1.0 + i$	< 1
2	0	0	$\pi$	50	$\frac{i}{\pi} \approx 0.318 i$	$-0.00524 - 0.0193i$	$-1.0 + \frac{i}{\pi}$ $-1.0 + \pi i$	< 9
3	1	0	2	100	$(0.435 - 0.351i) \cos \theta$	$(-0.00867 + 0.00498) \cos \theta$	$(0.0385 + 1.12i) \cos \theta$ $-1.2 + 1.6 i$	< 3
4	1	0	4.49	100	$(0.228i) \cos \theta$	$(-0.00867 + 0.00498) \cos \theta$	$(-0.976 - 0.239i) \cos \theta$ $-1.05 + 4.28i$	< 14
5	1	1	2	100	$(0.435 - 0.351i) \sin \theta \sin \xi$	$(-0.00867 + 0.00498) \sin \theta \sin \xi$	$(0.0385 + 1.12i) \sin \theta \sin \xi$ $-1.2 + 1.6 i$	not calculated

Parameters m and n refer to  
Eq. (26)

Table I.

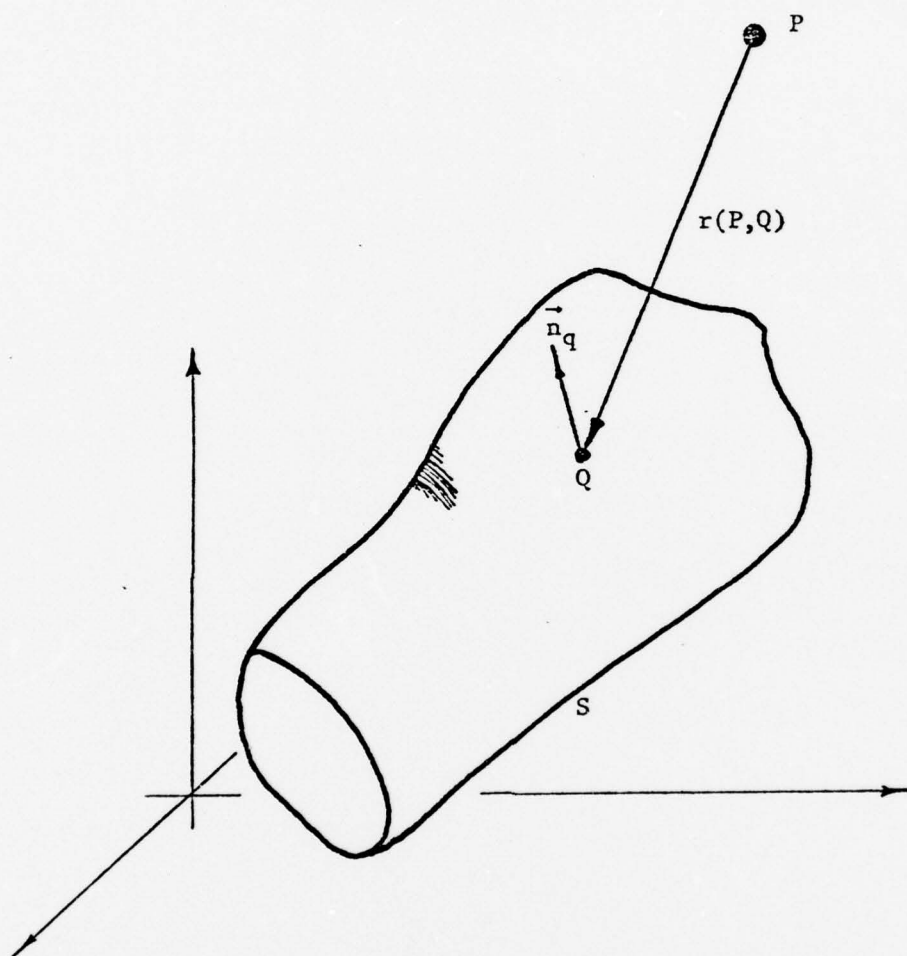
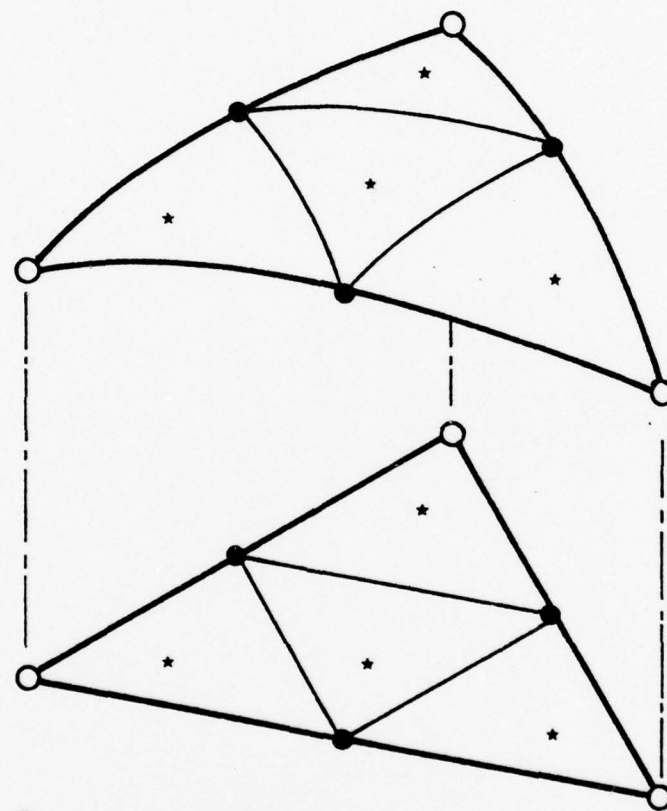


Figure 1. General Description of the Acoustic Radiation Problem.

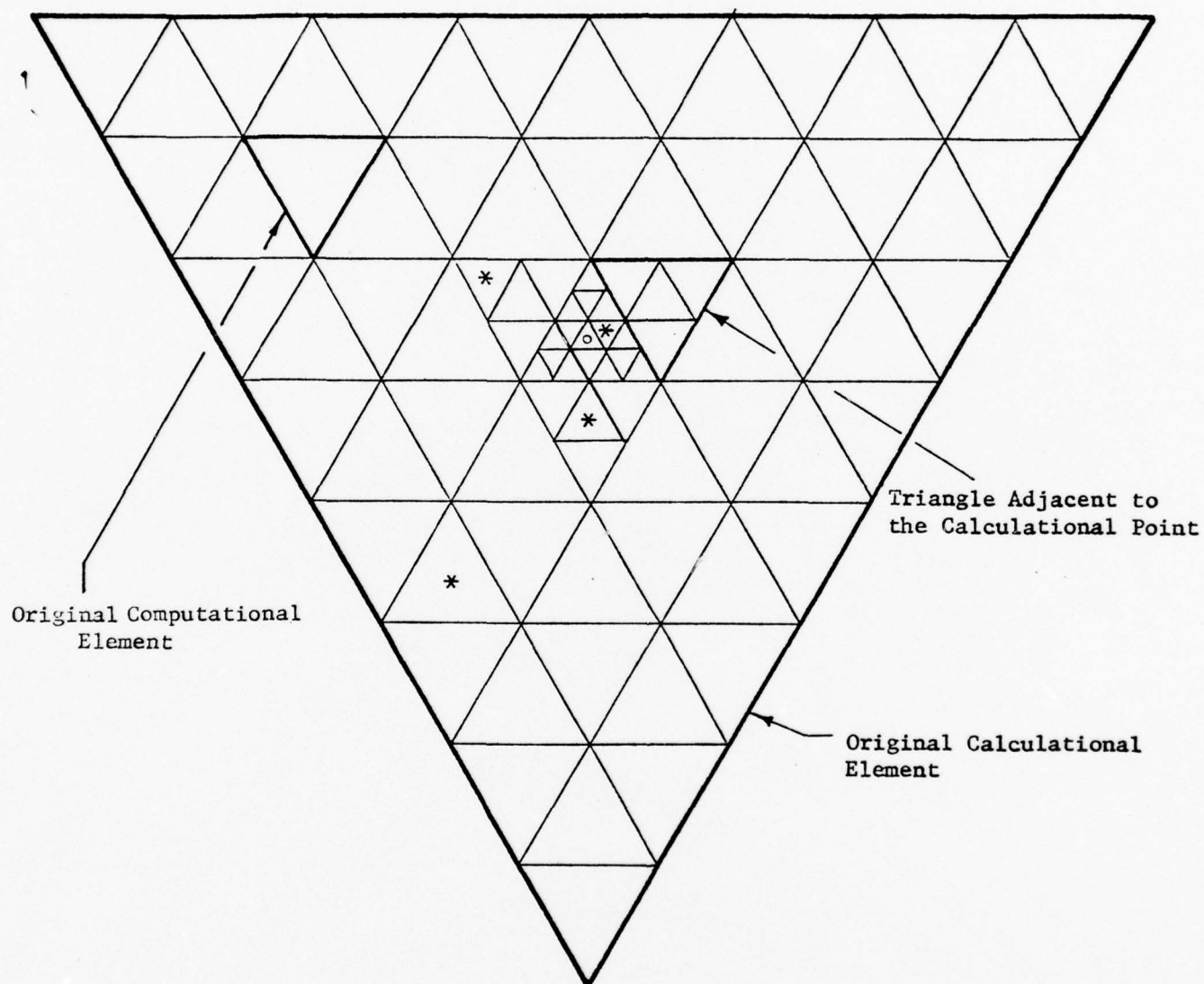


○ Already on Sphere

● Midpoint of Sides Projected to  
the Surface of the Sphere

★ Centroids of the Plane Triangles  
Projected to the Surface of the Sphere

Figure 2. Method of Dividing the Surface of the Sphere.



◦ The Calculational Point

\* A Computational Point

Figure 3. Division of the Surface of the Sphere Around a Calculational Point.

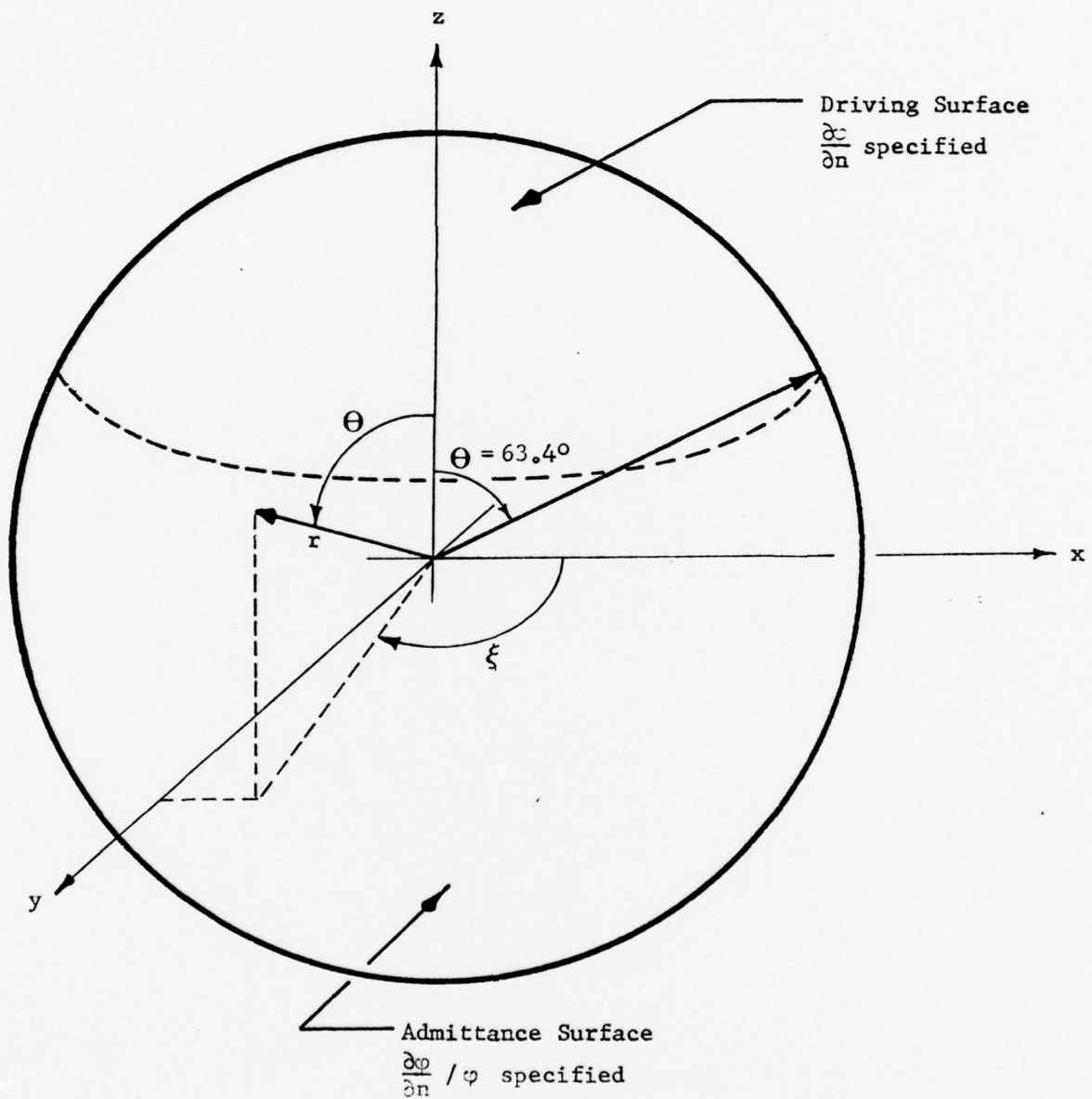


Figure 4. Specifications of Boundary Conditions on the Surface of the Sphere.

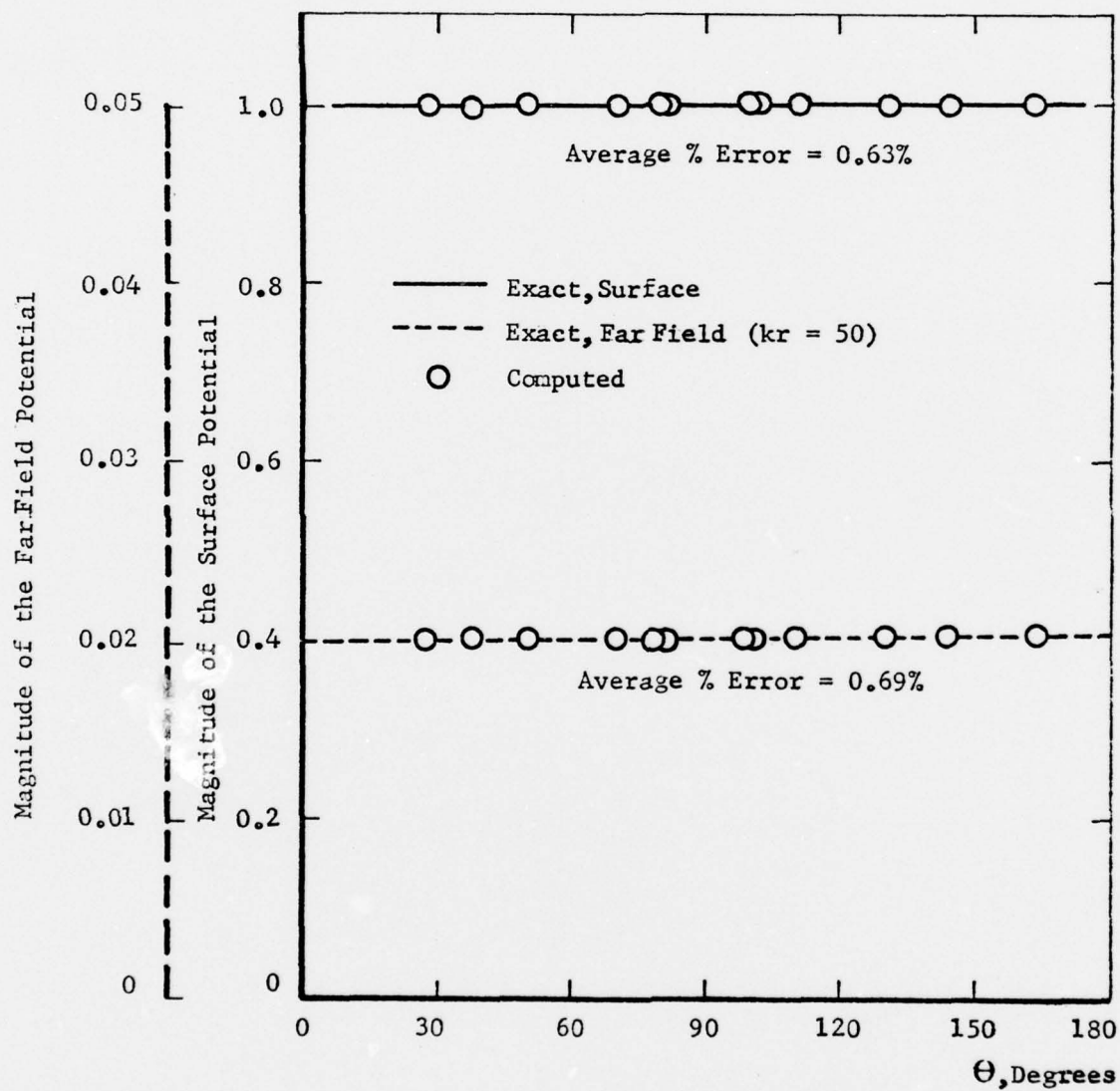


Figure 5. Exact and Calculated Values of  $|\varphi|$  for  $\varphi = h_0(r)$  on the Surface and in the Far Field of the Sphere.

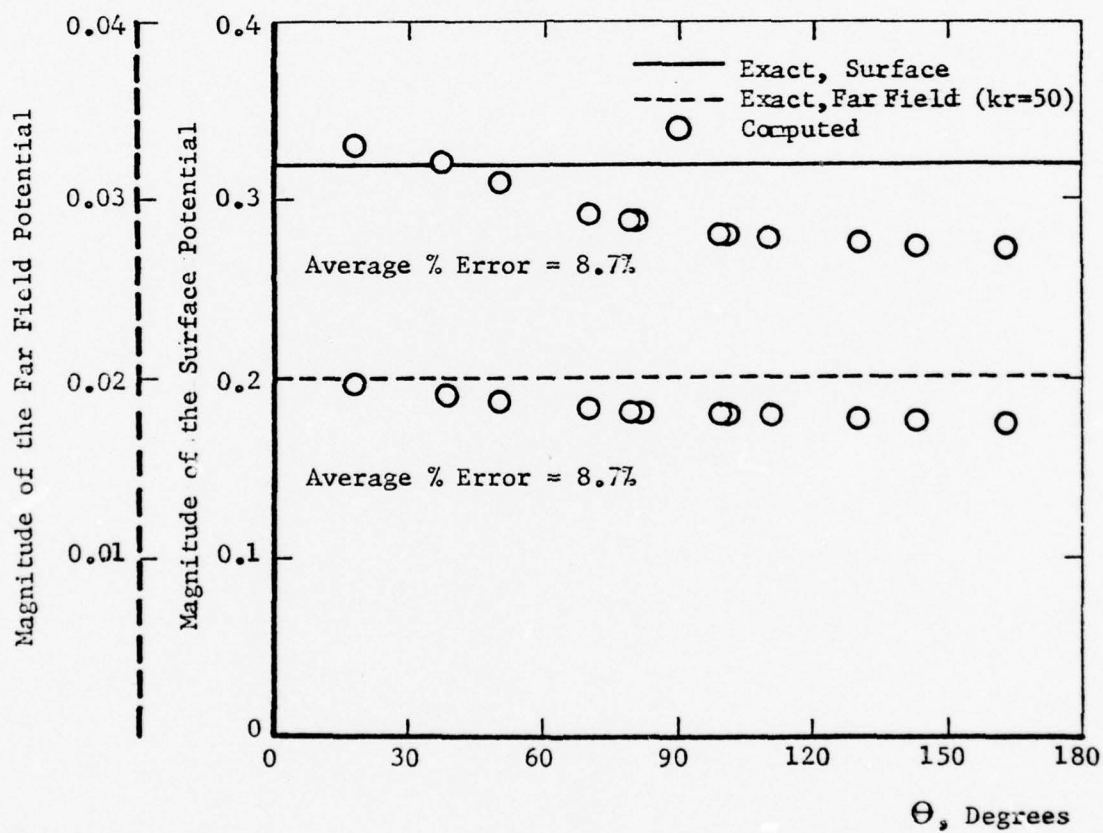


Figure 6. Exact and Calculated Values of  $|\varphi|$  for  $\varphi = h_0(\pi r)$  on the Surface and in the Far Field of the Sphere.

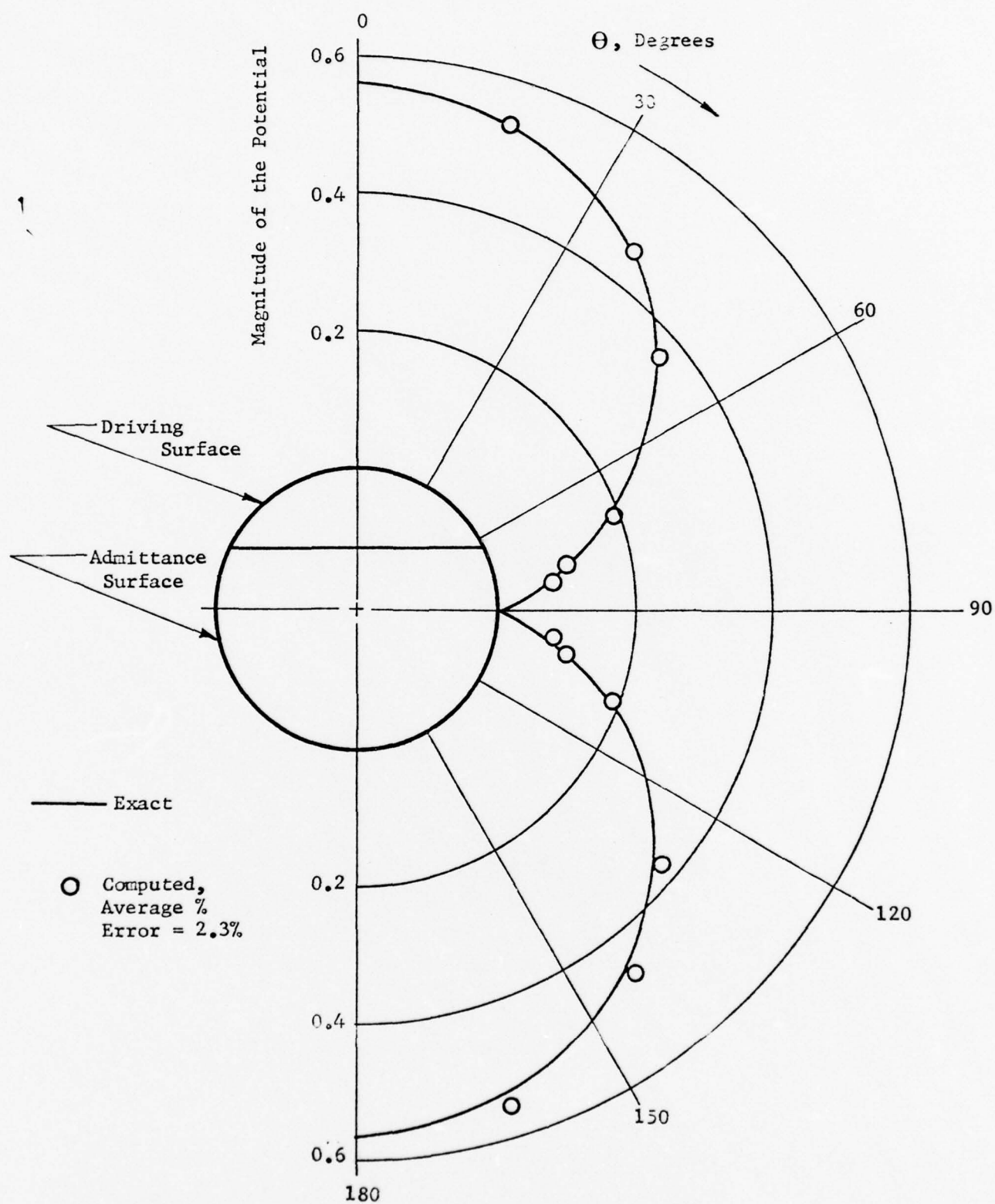


Figure 7. Exact and Calculated Values of  $|\phi|$  for  $\phi = h_1(2r) \cos \theta$  on the Surface of the Sphere.

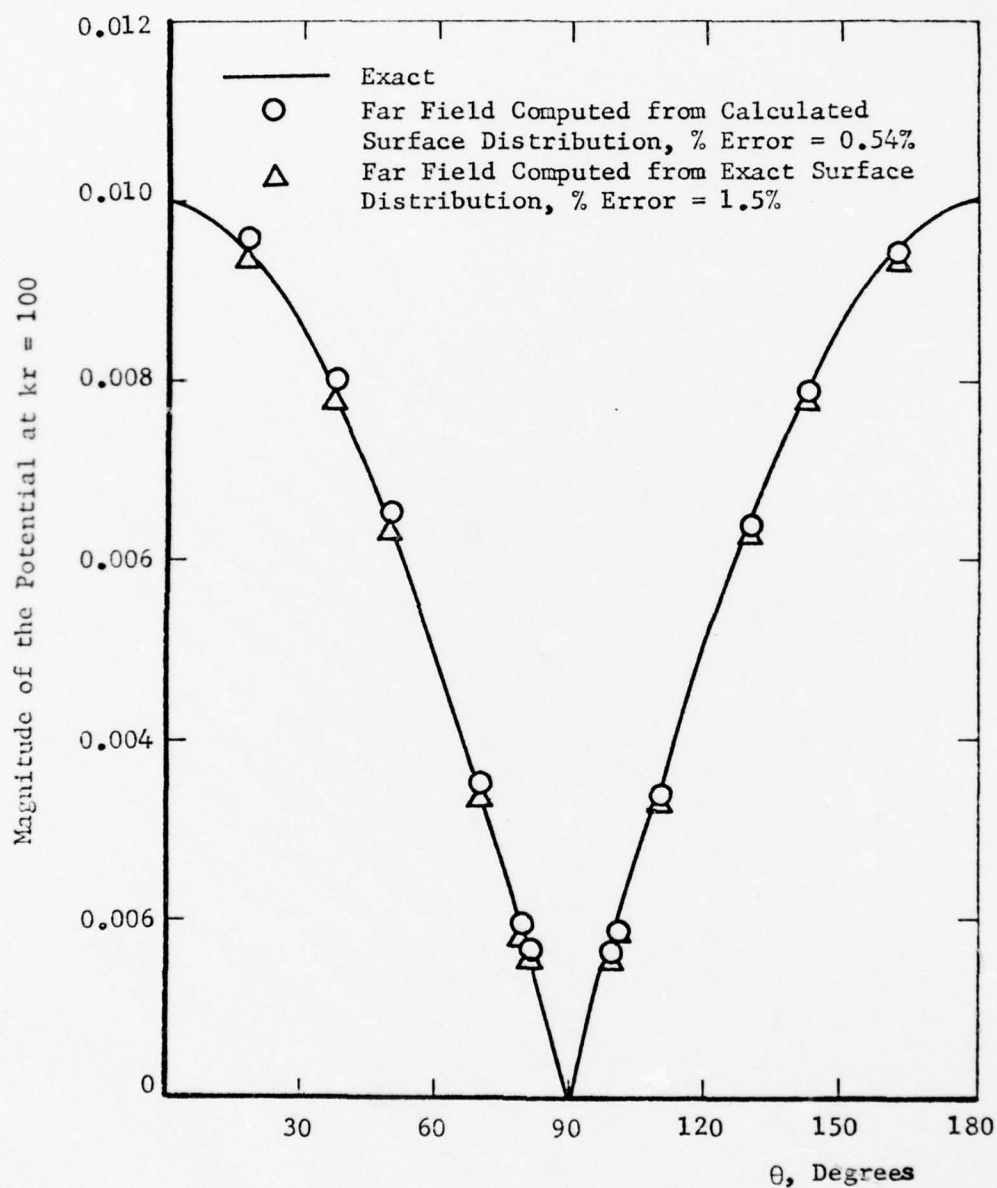


Figure 8. Exact and Calculated Values of  $|\varphi|$  using the Exact and Calculated Surface Distribution of  $\varphi$  for  $\varphi = h_1(2r) \cos \theta$  in the Far Field of the Sphere.

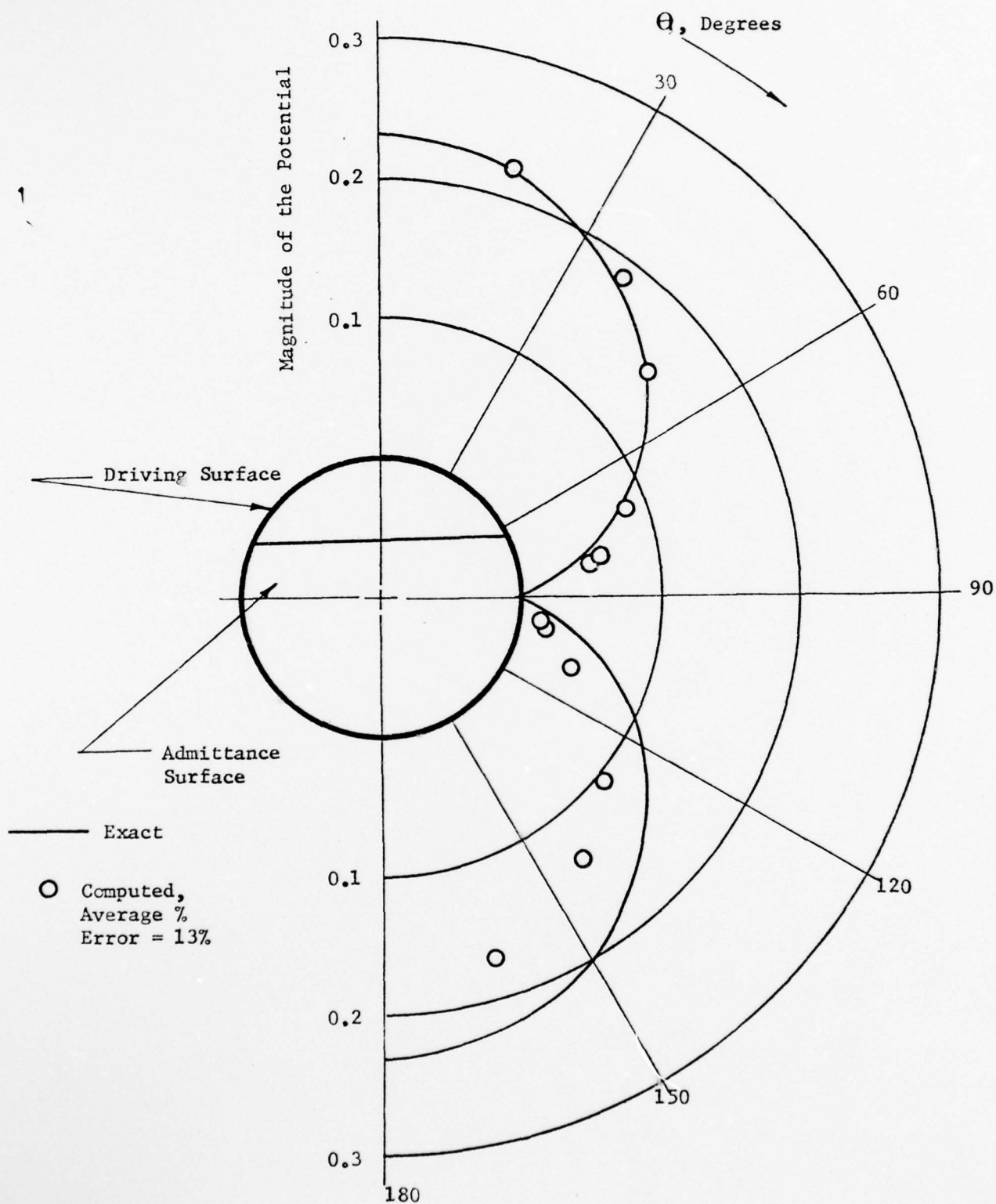


Figure 9. Exact and Calculated Values of  $|\varphi|$  for  $\varphi = h_1(4.49r) \cos \theta$  on the Surface of the Sphere.

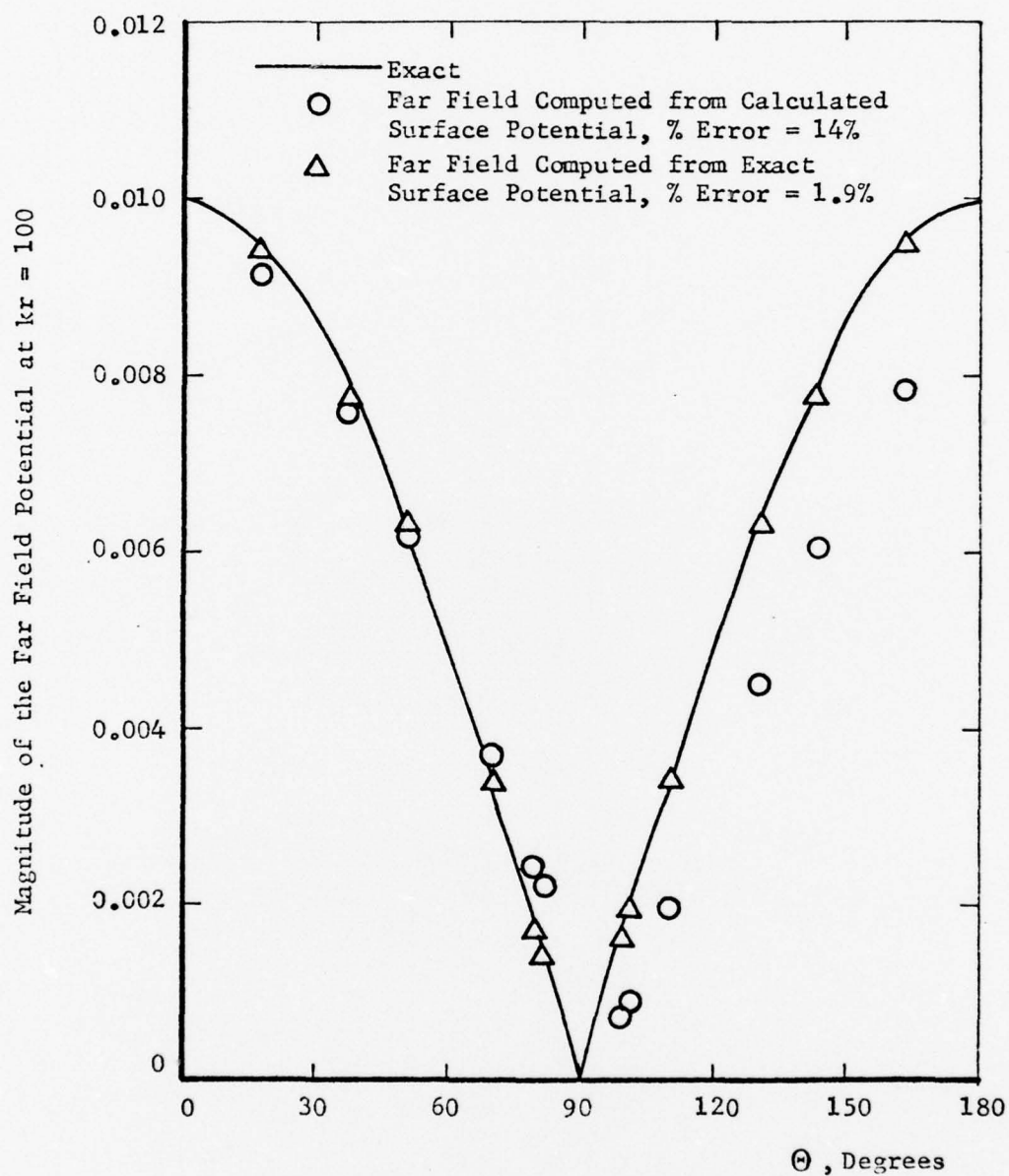


Figure 10. Exact and Calculated Values of  $|\varphi|$  using the Exact and Calculated Surface Distribution of  $\varphi$  for  $\varphi = h_1(4.49r) \cos \theta$  in the Far Field of the Sphere.

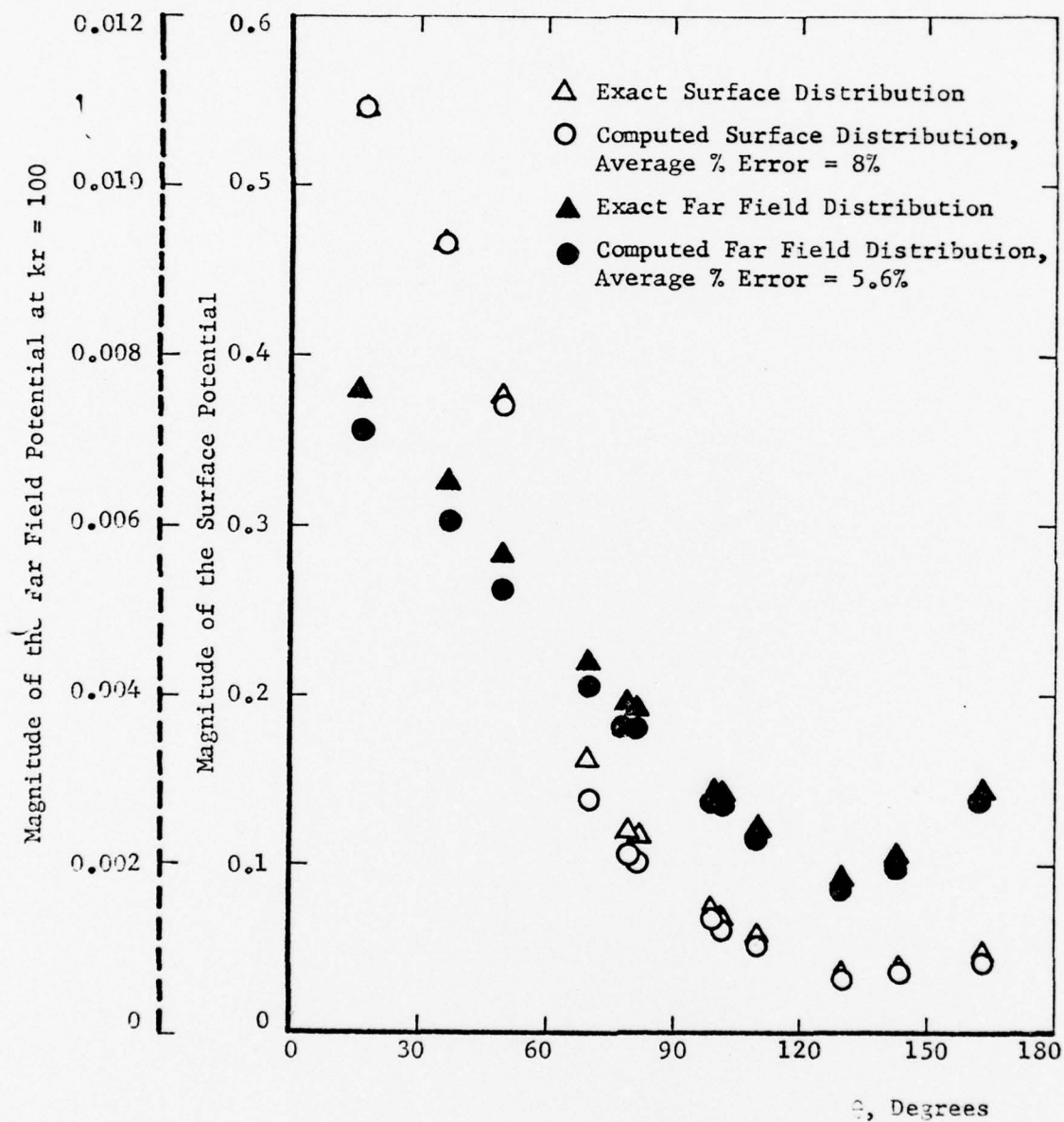


Figure 11. Exact and Calculated Values of  $|\phi|$  for a Hard Sphere with a Unit Driver ( $k = 2$ ) on the Surface and in the Far Field.

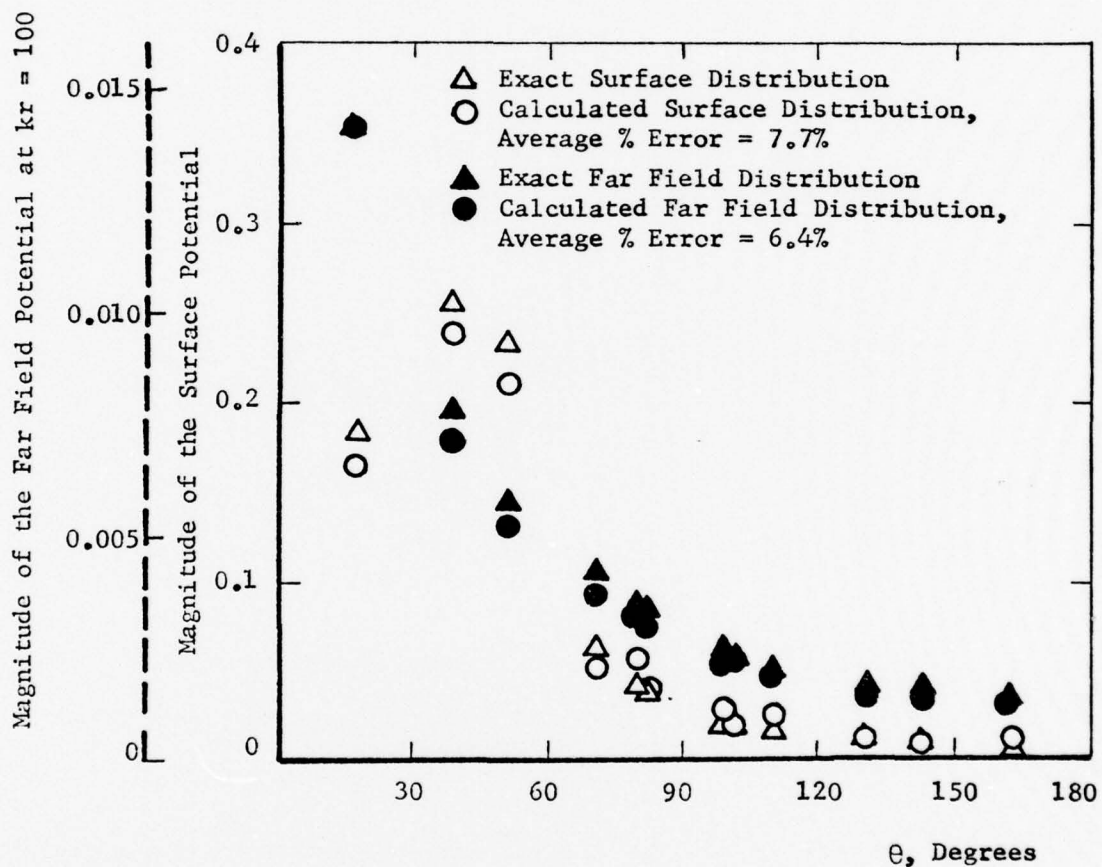


Figure 12. Exact and Calculated Values of  $|\phi|$  for a Hard Sphere with a Unit Driver ( $k = 5$ ) on the Surface and in the Far Field.

APPENDIX B

# PREDICTION OF THE SOUND FIELD RADIATED FROM AXISYMMETRIC SURFACES

W. L. Meyer\*, W. A. Bell,\*\* and B. T. Zinn\*\*\*

School of Aerospace Engineering  
Georgia Institute of Technology  
Atlanta, Georgia 30332

## Abstract

A general analytical method for determining the radiated sound fields from axisymmetric surfaces of arbitrary cross section with general boundary conditions is developed. The method is based on an integral representation of the external solutions of the Helmholtz equation valid at all wave numbers. The axisymmetric formulation of the problem reduces its solution to the numerical evaluation of line integrals by Gaussian quadrature. The applicability of the solution approach for both a sphere and finite cylinder is demonstrated by comparing the numerical results with exact analytical solutions for both discontinuous and continuous boundary conditions.

## I. Introduction

To reduce the noise radiated to the community from turbofan inlets, the effects of sound suppression material in the inlet and the spatial distribution of the sound source on the radiated sound levels and patterns must be determined. Analytical techniques for predicting these effects must be capable of dealing with general axisymmetric geometries and complicated boundary conditions which are encountered in multiply-lined inlets. To determine the radiated sound field, an additional requirement is that the methods be applicable to infinite domains. The objective of this paper is to develop a general analytical method for determining the radiated sound fields from axisymmetric surfaces of arbitrary cross section and with general boundary conditions.

The method used in this investigation is based on an integral form of the solutions of the Helmholtz equation.<sup>1-6</sup> With this formulation the acoustic potential anywhere external to the surface can be found once the potential distribution on the surface is known. Thus, to determine the radiated sound field the problem reduces to the determination of the distribution of the acoustic potential on the two-dimensional surface of the geometry under consideration instead of solving the Helmholtz equation in the surrounding infinite three dimensional domain.

It has been previously shown<sup>1-5</sup> that when applied to exterior sound radiation problems the solution technique fails to produce unique solutions at frequencies corresponding to interior eigenvalues of the geometries under consideration. Unless special precautions are taken, straight-forward numerical solutions of the developed integral equation at frequencies close to the eigenvalues of the internal problem produce large errors. A technique proposed by Burton and Miller<sup>4</sup> for avoiding this uniqueness problem and the associated numerical errors is used

in this investigation. This technique involves a reformulation of the "classical" integral equation and the solutions obtained are valid at all frequencies.

The resulting integral equation for the surface acoustic potential is solved numerically and, for axisymmetric geometries, the equation reduces to the evaluation of a line integral. Thus, the axisymmetric case can be reduced to an equivalent one-dimensional problem. This equation is discretized and the resulting system of algebraic equations is solved using complex Gauss-Jordan elimination. Since the coefficient matrix involves the free space Green's function, which becomes singular as two points on the surface approach one another, numerical techniques are presented which can deal with these singularities and yield accurate results. Gaussian integration is used to increase the accuracy of the solution without significant penalties in computer storage and time requirements. The applicability of the integral formulation and the accuracy of the numerical techniques are demonstrated by computing the surface and far field distributions of the acoustic potential on both a sphere and a finite cylinder. The numerical results are compared with known exact solutions generated by the separation of variables technique. Surfaces with spatially varying forcing functions and admittances are considered, for different tangential modes, to evaluate the capability of the integral approach to handle boundary conditions of a general nature. With the sphere, agreement between computed and exact results is to three significant figures. For the cylinder agreement is to two significant figures. The effect on the accuracy of discontinuous boundary conditions involving nonzero admittances over the surface and of the corners encountered in the cylindrical configuration are also presented.

## II. Theory

In this section the general three dimensional integral representation of the solutions of the Helmholtz equation is developed for application to radiation problems. This particular formulation yields unique solutions at all frequencies and does not have strong singularities which are difficult to handle numerically. The general integral equation is then specialized for axisymmetric geometries. A more detailed development is given in Ref. 5.

### General Theory

Beginning with the three dimensional Helmholtz equation which governs the spatial dependence of the acoustic field for sinusoidal oscillations

$$\nabla^2 \phi + k^2 \phi = 0 \quad (1)$$

where  $\phi$  is the acoustic potential and  $k$  is the wave number. The standard integral representation of the exterior solutions is found to be<sup>1,6</sup>

\* Assistant Research Engineer, Member AIAA

\*\* Research Engineer, Member AIAA

\*\*\* Regents' Professor, Associate Fellow, AIAA

$$\int_{S_q} \left( \varphi(Q) \frac{\partial G(P, Q)}{\partial n_q} - G(P, Q) \frac{\partial \varphi(Q)}{\partial n_q} \right) dS_q = 4\pi \varphi(P) \quad (2)$$

The term  $\frac{\partial}{\partial n_q}$  represents an outward normal derivative with respect to the body as shown in Fig. 1; that is

$$\frac{\partial \varphi(Q)}{\partial n_q} = \vec{\nabla}_q \varphi(Q) \cdot \vec{n}_q \quad (3)$$

Also,  $G(P, Q)$  is a fundamental three dimensional solution of the Helmholtz equation and is taken to be the free space Green's Function for a point source<sup>6</sup> defined as

$$G(P, Q) = \frac{e^{ikr(P, Q)}}{r(P, Q)} \quad (4)$$

From Eq. (3), if the acoustic potential and the normal acoustic velocity  $\frac{\partial \varphi(Q)}{\partial n_q}$  are known at each

point on the surface of the body then the acoustic potential may be calculated anywhere in the exterior domain.

To solve for the surface potential, the point P is moved to the surface of the body. Equation (2) then becomes

$$\int_{S_q} \left( \varphi(Q) \frac{\partial G(P, Q)}{\partial n_q} - G(P, Q) \frac{\partial \varphi(Q)}{\partial n_q} \right) dS_q = 2\pi \varphi(P) \quad (5)$$

if the surface of the body is sufficiently smooth. Introducing a modified admittance function defined as

$$Y(Q) \equiv \frac{\partial \varphi(Q)}{\partial n_q} / \varphi(Q) \quad (6)$$

Eq. (5) can be written as

$$\int_{S_q} \varphi(Q) \frac{\partial G(P, Q)}{\partial n_q} dS_q - \int_{S_{q1}} \varphi(Q) G(P, Q) Y(Q) dS_{q1} \quad (7)$$

$$= 2\pi \varphi(P) + \int_{S_{q2}} \frac{\partial \varphi(Q)}{\partial n_q} G(P, Q) dS_{q2}$$

$$\text{where } \int_{S_q} = \int_{q_1} + \int_{q_2}$$

If either the acoustic velocity or the admittance is known at each point on the surface of the body then the acoustic potential may be calculated at each point using Eq. (7).

Unfortunately this equation does not yield unique solutions when the wave number  $k$  is an internal eigenvalue of the body under consideration. Since these eigenvalues are not known a priori for general bodies the formulation cannot be relied upon to give consistently good results. There are many papers in the literature<sup>2,3,4</sup> dealing with this problem. The relative merits and shortcomings of the methods employed are discussed in detail in

Ref. 1.

The soundest approach from an analytical point of view is given by Burton and Miller<sup>4</sup> who have suggested the use of the differential forms of Eq. (5) which governs the spatial dependence of the acoustic velocity.

$$2\pi \frac{\partial \varphi(P)}{\partial n_p} = \int_{S_q} \left[ \varphi(Q) \frac{\partial^2 G(P, Q)}{\partial n_p \partial n_q} - \frac{\partial G(P, Q)}{\partial n_p} \frac{\partial \varphi(Q)}{\partial n_q} \right] dS_q$$

This equation can also be solved for  $\varphi(Q)$  once the normal velocity or admittance is specified at the surface. However, this equation has its own set of associated eigenvalues at which unique solutions cannot be obtained. Burton and Miller suggest taking a linear combination of the two equations to obtain

$$\begin{aligned} \int_{S_q} \left( \varphi(Q) \frac{\partial G(P, Q)}{\partial n_q} - G(P, Q) \frac{\partial \varphi(Q)}{\partial n_q} \right) dS_q \\ + \alpha \int_{S_q} \left( \varphi(Q) \frac{\partial^2 G(P, Q)}{\partial n_p \partial n_q} - \frac{\partial G(P, Q)}{\partial n_p} \frac{\partial \varphi(Q)}{\partial n_q} \right) dS_q \\ = 2\pi \left( \varphi(P) + \alpha \frac{\partial \varphi(P)}{\partial n_p} \right) \end{aligned} \quad (8)$$

Since the two sets of associated internal eigenvalues are mutually exclusive the linear combination of equations should yield unique solutions if the complex coupling constant  $\alpha$  is properly chosen. It is shown that  $\alpha$  must meet the following restrictions to guarantee that Eq. (8) yield unique solutions

$$\begin{aligned} \text{Im}(\alpha) \neq 0 & \quad k \text{ real or imaginary} \\ \text{Im}(\alpha) = 0 & \quad k \text{ complex} \end{aligned} \quad (9)$$

A problem arises in the numerical solution of Eq. (8) as the third term on the right hand side is strongly singular in its present form as the point Q approaches the point P on the surface of the body. Meyer, Bell and Zinn<sup>5</sup> have shown that this difficulty can be overcome by the proper interpretation of this singular term. Employing a vector transformation<sup>7</sup> and taking the Cauchy Principle Value Eq. (8) is shown to be equivalent to

$$\begin{aligned} \int_{S_q} \left( \varphi(Q) \frac{\partial G(P, Q)}{\partial n_q} - G(P, Q) \frac{\partial \varphi(Q)}{\partial n_q} \right) dS_q \\ + \alpha \int_{S_q} (\varphi(Q) - \varphi(P)) \frac{\partial^2 G(P, Q)}{\partial n_p \partial n_q} dS_q \\ - \alpha \varphi(P) \int_{S_q} (\vec{n}_p \cdot \vec{n}_q) (ik)^2 G(P, Q) dS_q \\ - \alpha \int_{S_q} \frac{\partial G(P, Q)}{\partial n_p} \frac{\partial \varphi(Q)}{\partial n_q} dS_q = 2\pi \left( \varphi(P) + \alpha \frac{\partial \varphi(P)}{\partial n_p} \right) \end{aligned} \quad (10)$$

All of the terms in Eq. (10) are now regular and therefore are directly integrable; however, all the integrands are oscillatory and singular so that care must be taken in their numerical approximation.

#### Axisymmetric Formulation

When dealing with a body of revolution as shown in Fig. 2 an axisymmetric formulation of the problem is advantageous.<sup>8</sup> This being the case an element of area becomes

$$dS_q = \tau dS d\theta$$

where  $S$  is the distance along the perimeter of the surface in the  $\tau$ - $z$  plane.

Assuming an acoustic velocity distribution of the form

$$\frac{\partial \varphi}{\partial n} = v(S) \cos m \theta \quad (12)$$

and defining a potential function

$$\Phi(S) \equiv \frac{\varphi}{\cos m \theta} \quad (13)$$

Eq. (10) becomes

$$\begin{aligned} & \int_{S_q} \int_{S_p} \Phi(S_q) \frac{\partial G(P,Q)}{\partial n_q} \cos m \theta_q dS_q \\ & - \alpha \Phi(S_p) \int_{S_q} \int_{S_p} G(P,Q) (ik)^2 (n_p \cdot n_q) dS_q \\ & + \alpha \int_{S_q} \int_{S_p} [\Phi(S_q) \cos m \theta_q - \Phi(S_p)] \frac{\partial^2 G(P,Q)}{\partial n_p \partial n_q} dS_q \\ & - \int_{S_q} \int_{S_p} v(S_q) G(P,Q) \cos m \theta_q dS_q \\ & - \alpha \int_{S_q} \int_{S_p} v(S_q) \frac{\partial G(P,Q)}{\partial n_p} \cos m \theta_q dS_q \\ & = 2\pi [\Phi(S_p) + \alpha v(S_p)] \end{aligned} \quad (14)$$

In the above equation  $\theta_p$  has been assumed to be zero so that  $\cos m \theta_p = 1$ .

Now, three sets of functions are defined:

#### Influence Functions

$$\begin{aligned} I_1(S_p, S_q) &= 2 \int_0^\pi G(P,Q) \cos m \theta_q d\theta_q \\ I_2(S_p, S_q) &= 2\alpha \int_0^\pi \frac{\partial G(P,Q)}{\partial n_p} \cos m \theta_q d\theta_q \end{aligned} \quad (15)$$

#### Kernel Functions

$$K_1(S_p, S_q) = 2 \int_0^\pi \frac{\partial G(P,Q)}{\partial n_q} \cos m \theta_q d\theta_q \quad (16)$$

$$K_2(S_p, S_q) = 2\alpha \int_0^\pi \frac{\partial^2 G(P,Q)}{\partial n_p \partial n_q} \cos m \theta_q d\theta_q$$

#### Forcing Functions

$$F_1(S_p, S_q) = 2\alpha \int_0^\pi G(P,Q) (ik)^2 (n_p \cdot n_q) d\theta_q \quad (17)$$

$$F_2(S_p, S_q) = 2\alpha \int_0^\pi \frac{\partial^2 G(P,Q)}{\partial n_p \partial n_q} d\theta_q$$

Substituting Eqs. (15)-(17) into Eq. (14) gives

$$\begin{aligned} & \int_0^\ell \Phi(S_q) \{K_1(S_p, S_q) + K_2(S_p, S_q)\} dS_q \\ & - \Phi(S_p) \int_0^\ell \{F_1(S_p, S_q) + F_2(S_p, S_q)\} dS_q \\ & - \int_0^\ell v(S_q) \{I_1(S_p, S_q) + I_2(S_p, S_q)\} dS_q \\ & = 2\pi [\Phi(S_p) + \alpha v(S_p)] \end{aligned} \quad (18)$$

where  $\ell$  is the length of the generating line of the surface of revolution. The  $S$ - $\theta$  coordinate directions have now been effectively uncoupled so that the problem has been reduced to the evaluation of line integrals in the coordinate directions on the surface of the body. This formulation does not restrict the form or type of boundary conditions on the body; it merely assumes that the boundary conditions can be represented by a sum (expanded in a set) of tangential modes.

#### III. Results

Numerical results have been obtained for a sphere and cylinder using the numerical technique described in Ref. 9. Basically, this method consists of first specifying the  $\tau$ - $z$  coordinates and the normal vector at each point on the surface. From these quantities the distances  $r$  and the normal derivatives  $\frac{\partial}{\partial n}$  can be obtained. The integral in Eq. (18) is  $\frac{\partial}{\partial n_q}$  then separated into  $n$  integrals taken over subintervals of length  $\ell/n$ . The acoustic potential is assumed constant over each subinterval and the integrations are performed numerically using a four-point Gauss-Legendre quadrature in the  $\tau$ - $z$  plane. A twenty-point Gauss-Legendre quadrature formula is used in the circumferential direction.

Exact results were obtained using separation of variables.<sup>6</sup> To eliminate the need for evaluating the resulting infinite series, the normal velocity and admittance distributions were selected so that only one term in the series remains.

To investigate the effect of the coupling constant  $\alpha$  in Eq. (18), the surface potential distributions were obtained for  $\alpha = 0, i$ , and  $i/k$  for twenty points on the sphere. The exact solution assumed for this case is

$$\varphi(P) = \frac{e^{ikr(P)}}{r(P)} \quad (19)$$

where  $r$  is the distance from the origin to a point  $P$  on the surface. As shown in Fig. 3, with  $\alpha = 0$  the computed magnitudes of the acoustic potential are in error by 12 per cent at wave numbers close to the internal eigenfrequencies of  $\pi, 2\pi$  and  $3\pi$ . These results are those that would be obtained from Eq. (5). The relatively large errors are expected from the analysis of Burton<sup>1</sup> and from previous investigations using Eq. (5).<sup>2,5</sup> Burton proves that setting the imaginary part of  $\alpha$  nonzero guarantees unique solutions when Eq. (18) is used. Although the maximum error is reduced for  $\alpha = i$  to less than 4 per cent when the nondimensional frequency  $k$  is less than seven, significant errors are still evident at the higher frequencies as shown in Fig. 3.

In this study consistently good results are obtained only when  $\alpha = i/k$ . In Fig. 3, the computed and exact results with  $\alpha = i/k$  agree to three significant figures. The reason for this behavior is currently under investigation; however, for all the cases presented hereafter this value of  $\alpha$  is chosen and the exact surface distribution is given by Eq. (19) when  $m = 0$ .

A problem of more practical importance is the finite axisymmetric duct since this surface approximates an engine configuration. The surface potential distributions are presented in Fig. 4 for a zero admittance everywhere on the surface. The velocity distribution is specified over the entire surface and the potential given by Eq. (19) has a magnitude independent of frequency and a phase linearly proportional to the frequency. In Fig. 4 the magnitude and phase are plotted against the distance along the perimeter  $S$ . The largest errors in the magnitude of the potential of about 10 percent occur on the ends of the cylinder and at the corners. The results at the ends can be improved without increasing the number of points by area weighting rather than by taking equidistant points along the perimeter. The errors at the corners are caused by the discontinuous normal derivative in going from the cylinder to the end. The errors in the phase are less than four per cent in all cases. The errors in magnitude increase with increasing frequency, but even when  $k = 10$  the numerical results are within 10 per cent of the exact solutions.

In most practical problems the boundary conditions are discontinuous with the acoustic velocity or potential specified over part of the surface and the admittance over the rest. To determine the effect of the discontinuities on the numerical results, a cylinder with the velocity specified on the ends and the admittance specified in the center was investigated and the results are presented in Fig. 5. Although the errors of the numerical results for this case are increased compared with the errors shown in Fig. 4, the errors are within 10 per cent for values of  $k$  less than 5. However, when  $k = 10$  errors of up to 40 per cent in the magnitude of the potential are encountered close to the discontinuity in the boundary condition. This result suggests

that more points need to be taken at higher frequencies with discontinuous boundary conditions present.

At higher tangential modes, the variation in the circumferential direction behaves as  $\cos m\theta$  where  $m = 0, 1, 2, \dots$ . To check the numerical integration scheme in the circumferential direction, the surface acoustic potential was computed for  $m = 1$  and  $m = 2$ . The results are presented in Fig. 6 for  $k = 2$  with the velocity specified and the admittance zero everywhere on the surface. The computed and exact results are in agreement to within two per cent for both  $m = 1$  and  $m = 2$ .

It has been shown<sup>5</sup> that once the surface potential has been accurately computed, the far field can be determined to at least the accuracy of the surface potential. This result is confirmed by the data presented in Fig. 7 for a cylinder with the velocity specified everywhere on the surface at  $k = 2$ . The results at 20 radii from the surface are in agreement with exact results to within one per cent even though the surface errors at some points is above two per cent. Data in Fig. 8 show that accurate results are obtained at distances greater than one integration stepsize from the surface. At closer distances errors from the numerical evaluation of the singularity in the Green's function defined by Eq. (4) leads to large errors.

#### IV. Summary and Conclusions

An integral solution of the Helmholtz equation is developed for use in acoustic radiation problems. Unlike previous formulations which give poor results at frequencies corresponding to eigenfrequencies of the surface under consideration, the formulation used in this study is valid at all frequencies. The surface potentials computed numerically for a sphere and cylinder using 20 points along the perimeter are accurate to within ten per cent for nondimensional frequencies  $ka$  of from one to ten where  $k$  is the wave number and  $a$  is the radius of the sphere or cylinder. For discontinuous boundary conditions, the numerical and exact values are in agreement to within 10 per cent for  $ka < 5$ . At higher frequencies the results are as much as 40 per cent in error at the point of discontinuity which suggests taking more points in evaluating the integral Helmholtz equation to increase the accuracy when discontinuous boundary conditions are specified. At distances greater than the numerical integration stepsize, the far field results are at least as accurate as the corresponding surface potential solutions.

#### References

1. Burton, A. J., "The Solution of Helmholtz' Equation in Exterior Domains using Integral Equations," NPL Report NAC 30, National Physical Laboratory, Teddington, Middlesex, Jan. 1973.
2. Schenck, H. A., "Improved Integral Formulation for Radiation Problems," *Journal of the Acoustical Society of America*, Vol. 44, No. 1, Jan. 1968, pp. 41-58.
3. Ursell, F., "On the Exterior Problems of Acoustics," *Proceedings of the Cambridge Philosophical Society*, Vol. 74, 1973, pp. 117-125.
4. Burton, A. J. and Miller, G. F., "The Application of Integral Equation Methods to the Numerical Solutions of Some Exterior Boundary Value

Problems," Proceedings of the Royal Society of London, A323, 1971, pp. 201-210.

5. W. L. Meyer, W. A. Bell and B. T. Zinn, "Integral Solutions of Three Dimensional Acoustic Radiation Problems," to be published in the Journal of Sound and Vibration.
6. Morse, P. M. and Ingard, K. U., Theoretical Acoustics, McGraw-Hill, New York, 1969, Chapter 7.
7. Stallybrass, M. P., "On a Pointwise Variational Principle for the Approximate Solution of Linear Boundary Value Problems," Journal of Mathematics and Mechanics, Vol. 16, No. 11, May 1967, pp. 1247-1286.
8. Andreasen, M. G., "Scattering from Bodies of Revolution," IEEE Transactions on Antennae and Propagation, March 1965, pp. 303-310.
9. Bell, W. A., Meyer, W. L., and Zinn, B. T., "Predicting the Acoustics of Arbitrarily Shaped Bodies Using an Integral Approach," AIAA Journal, Vol. 15, No. 6, June 1977, pp. 813-820.

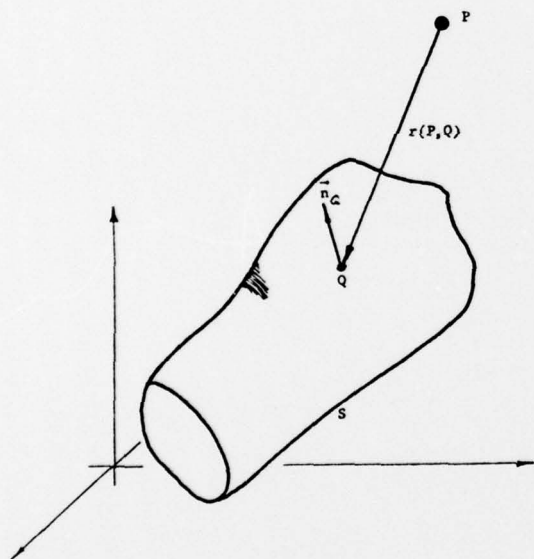


Figure 1. General Description of the Acoustic Radiation Problem

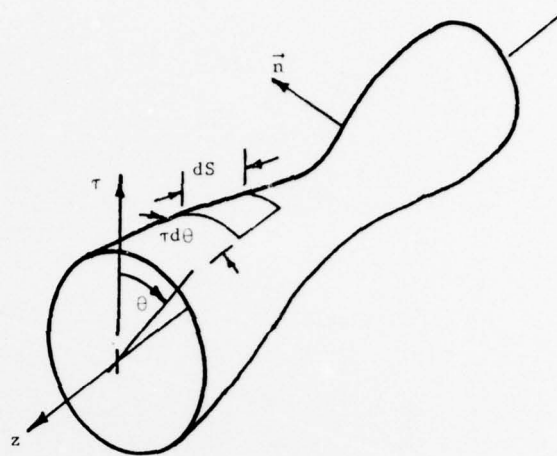


Figure 2. Cylindrical Surface Geometry.

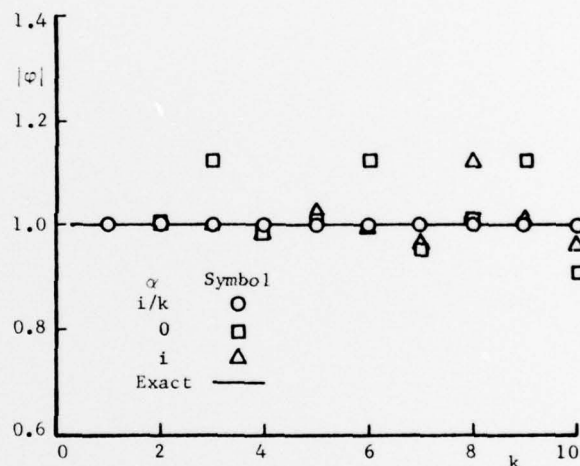


Figure 3. Effect of Coupling Constant  $\alpha$  on Computed Surface Potential for a Sphere of Unit Radius with 20 Points.

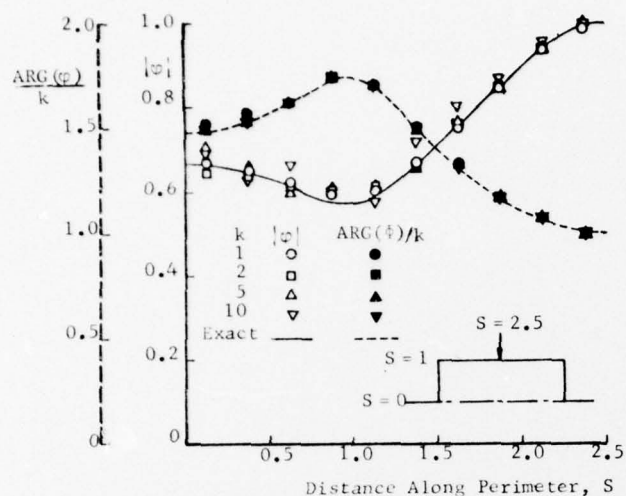


Figure 4. Dependence of the Computed Surface Potential for a Finite Cylinder with a Zero Admittance and Nonzero Normal Velocity Everywhere on the Surface with 20 Points.

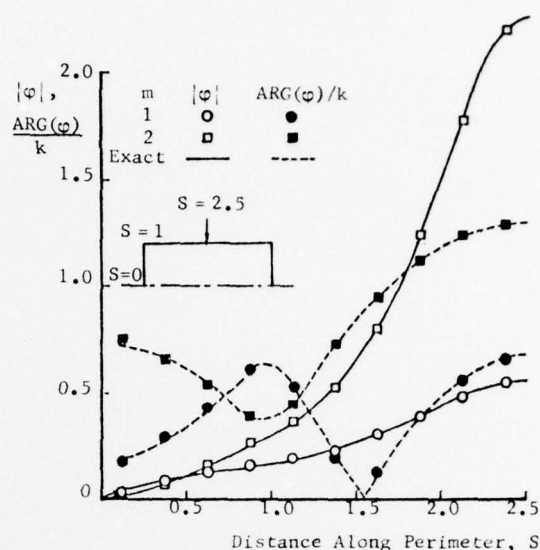


Figure 6. Computed Surface Potential for a Cylinder at the First and Second Tangential Modes for  $k = 2$  and 20 Points.

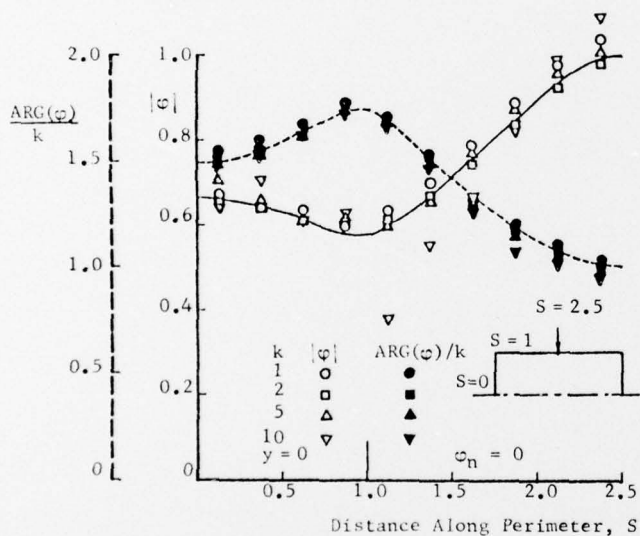


Figure 5. Effect of Discontinuous Boundary Conditions on the Computed Surface Potential for a Cylinder-20 Points.

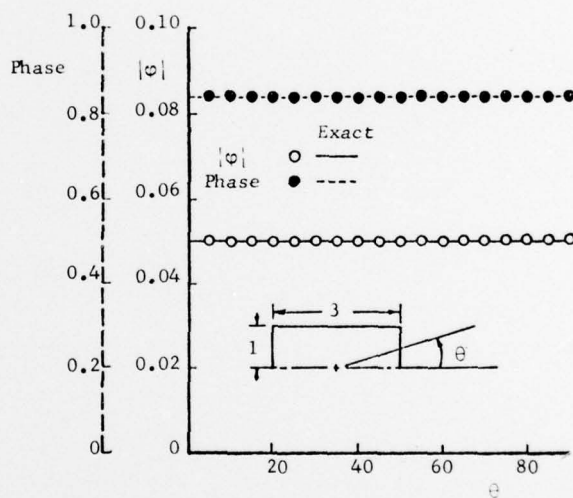


Figure 7. Computed Far Field Potential Distribution for a Cylinder at  $k = 2$ ,  $m = 0$ , and 20 Radii from the Center of the Cylinder.

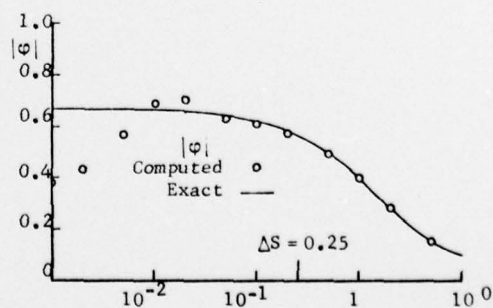


Figure 8. Dependence of the Far Field Solution of a Cylinder upon the Distance from the Surface for  $k = 2$  and  $m = 0$ .

APPENDIX C

## Predicting the Acoustics of Arbitrarily Shaped Bodies Using an Integral Approach

William A. Bell,\* William L. Meyer,† and Ben T. Zinn‡  
*Georgia Institute of Technology, Atlanta, Ga.*

An integral solution of the Helmholtz equation is developed for predicting the acoustic properties of arbitrarily shaped bodies. With the integral formulation, the acoustic potentials at the surface are solved independently of the internal acoustic field which, effectively, reduces the dimensionality of the problem by one. Considerable reductions in computation time and storage requirements are thus achieved. Efficient numerical techniques for solving the resulting algebraic equations are presented. Numerical results obtained for the two-dimensional problems of a circle and a rectangle agree to within one percent with available exact solutions. The modes of a star-shaped configuration and a duct with a right-angle bend are also determined to demonstrate the applicability of this method to complicated geometries and general boundary conditions. The acoustic properties of a sphere are investigated using an axisymmetric formulation. With the axisymmetric formulation the numerical and exact results agree to three significant figures.

### I. Introduction

THE prediction of the acoustics of arbitrarily shaped bodies has a variety of applications in aerospace engineering. Among them are the determination of the internal and radiated sound fields from airbreathing propulsion systems and the investigation of the stability limits of rocket combustors. These studies are concerned with obtaining solutions to the Helmholtz equation, which is derived from the wave equation when a sinusoidal time dependence is assumed and which describes the spatial dependence of the oscillations. This equation is included in most standard texts on differential equations of mathematical physics (Ref. 1, Ch. 11) and has been extensively studied in both differential and integral form. The differential form is currently the most widely used.

In differential form, solutions of the Helmholtz equation can be obtained by separation of variables.<sup>1,2</sup> This method involves series expansions of the solutions in terms of eigenfunctions of the system. Although this technique has been successfully applied to several practical problems in duct wave propagation,<sup>3-9</sup> it has the following limitations: 1) the series expansions often involve special functions which are difficult to compute; 2) at high frequencies and at the boundaries the series are slowly convergent—therefore, a large number of terms in the series must be retained to ensure accurate results, which often requires excessive computation time; 3) this method can only be used with special coordinate systems and boundary conditions for which the separation of variables can be applied. At present only eleven suitable coordinate systems are known (Ref. 1, p. 513ff).

For arbitrarily shaped bodies, the differential form of the Helmholtz equation can be solved by writing the equation in terms of finite differences (Ref. 1, p. 703ff). Unlike separation of variables, this technique is not limited to ducts with simple geometries. A typical application of finite differences is given by Wynne and Plumblee<sup>10</sup> who solved for the transverse eigenvalues and eigenfunctions of an annular duct with lined walls. This technique involves the simultaneous solution of the acoustic potential value at every point within the duct. Once the potential values are known,

the acoustic pressure and velocity can then be determined. To obtain sufficient accuracy, fine grid sizes must be used which necessitates large computer storage requirements. This drawback was noted by Baumeister,<sup>11</sup> Baumeister and Rice,<sup>12</sup> and Alfredson<sup>13</sup> who used this technique in studies of duct wave propagation. Because of the storage requirements this technique has mainly been applied to two-dimensional problems. For three-dimensional problems numerical methods capable of handling large matrices must be used which require considerable computer time and computational effort.<sup>14</sup> This technique is also impractical in radiation problems which involve infinite domains.

To avoid the limitations of the differential formulation, the integral approach is employed in this study. The integral approach has been successfully applied to a wide range of acoustic problems. In determining the sound radiation field from vibrating surfaces, integral techniques have been widely used.<sup>15-18</sup> For example, Chen and Schweikert<sup>15,16</sup> employed this method to determine the radiation sound patterns for three-dimensional shapes with mixed boundary conditions. To check the accuracy of the results, they computed the radiated field produced by a piston vibrating on a sphere. For this problem an exact solution exists<sup>3</sup> and compares favorably with the numerical results. The integral formulation is also used to solve the problem of scattering by arbitrary shapes.<sup>15,21</sup> Banaugh and Goldsmith, for example, used this technique to investigate the effect of surface shape<sup>19</sup> on scattered sound fields. By applying this method to a circular cylinder, for which exact solutions are available,<sup>3,4</sup> and comparing the exact and numerical solutions, Banaugh and Goldsmith demonstrated the accuracy of the integral solution scheme. Although this method is capable of handling mixed boundary conditions, only surfaces with rigid boundaries were considered in Ref. 19. The effect of mixed boundary conditions was included in studies by Liu and Martenson<sup>22</sup> and Quinn<sup>23</sup> of the internal acoustic pattern of lined ducts with arbitrary shapes. Comparison of the theoretical predictions with experimental data showed generally good agreement. Unpublished work by Zinn and Gaylord<sup>24</sup> demonstrated the applicability of the integral formulation for the determination of the natural frequencies and modes for two-dimensional shapes. In this study the accuracy of the technique was determined by comparing the natural frequencies and mode shapes with available exact solutions for a two-dimensional cylinder with rigid walls. The agreement is to within four decimal places which is two-orders-of-magnitude more accurate than previous results

Presented as Paper 76-494 at the 3rd AIAA Aero-Acoustics Conference, Palo Alto, Calif., July 20-23, 1976; submitted Aug. 2, 1976; revision received March 15, 1977.

Index categories: Noise; Aeroacoustics.

\*Instructor, Member AIAA.

†Research Associate.

‡Regents' Professor, Associate Fellow AIAA.

obtained by solving the differential Helmholtz equations using finite differences.<sup>10</sup> In another study by Tai and Shaw,<sup>25</sup> the integral method was applied to a right triangle. The resulting eigenfrequencies compared with exact solutions to within 5% and the maximum deviation between the numerically computed and exact potential fields was less than 1%.

To demonstrate the accuracy and the versatility of the integral solution technique, results are obtained for several acoustic problems involving a variety of geometries. To obtain a solution, the integral equation is first discretized to form a system of algebraic equations which are then solved for the acoustic potential at discrete points on the boundary. From these values the rest of the sound field is obtained. Methods for increasing the numerical accuracy by use of Gaussian quadrature and other numerical integration methods are presented and discussed. The first problem considered is the numerical evaluation of the resonant frequencies and natural modes of two-dimensional circular, rectangular, and star configurations. Exact and numerical values are compared for the circle and rectangle. The next problem considered is a two-dimensional duct with a right-angle bend with a sound source at one end and sound absorption treatment at various locations along the duct. The results are compared with finite difference solutions. These studies demonstrate the applicability of the integral formulation to complicated geometries and general boundary conditions. The next problem considered is the two-dimensional radiation problem of a piston set in a right circular cylinder. Again, the exact and numerical acoustic fields are computed and compared. Finally, a three-dimensional problem of determining the acoustic properties of a sphere is considered. The internal field is obtained using an axisymmetric formulation.

## II. Governing Equations

The integral formulations of the wave equation for internal and radiation acoustic problems are developed in this section for two and three dimensions. The boundary conditions generally encountered in practical problems are then discussed. For clarity, only a brief account of the derivation of the basic equations will be given in this section. For a more detailed and rigorous development, Refs. 26 through 29 can be consulted.

Assume a frictionless, homogeneous gas, and let  $\rho_0$  and  $p_0$  be the density and pressure of the fluid at rest. Representing the acoustic pressure and particle velocity at a time  $t$  by  $p$  and  $u$ , Euler's equation for the conservation of momentum gives

$$\rho_0 \frac{\partial u}{\partial t} + \nabla p = 0 \quad (1)$$

The continuity equation yields the relationship

$$\frac{\partial p}{\partial t} + \rho_0 c_0^2 \nabla \cdot u = 0 \quad (2)$$

where  $c_0$  is the speed of sound. By defining an acoustic potential function  $\Psi$  such that

$$u = \nabla \Psi \quad (3)$$

Equation (1) provides the relation

$$p = -\rho_0 \frac{\partial \Psi}{\partial t} \quad (4)$$

and Eq. (2) results in the classical wave equation

$$\nabla^2 \Psi - \frac{1}{c_0^2} \frac{\partial^2 \Psi}{\partial t^2} = 0 \quad (5)$$

The wave equation can also be written in terms of  $p$  and  $u$ , but it is more convenient to work with an acoustic potential function, from which both the acoustic pressure and particle velocity can readily be obtained.

Equation (5) is the wave equation for a general time dependence and can be written in integral form and solved by using retarded potentials.<sup>21,28</sup> However, for most practical problems a sinusoidal time dependence can be assumed which simplifies the problem considerably. Assume

$$\Psi(r, t) = \phi(r) e^{i\omega t} \quad (6)$$

Substituting Eq. (6) into Eq. (5) gives the Helmholtz equation

$$\nabla^2 \phi + k^2 \phi = 0 \quad (k = \omega/c_0) \quad (7)$$

which can be solved by simpler methods not involving the use of retarded potentials.

### Integral Formulation

To obtain an integral formulation of the Helmholtz equation, consider the problem shown in Fig. 1. Applying Green's theorem to the Helmholtz equation<sup>1,28,29</sup> gives the following integral relation

$$\int_{\Gamma} \left[ \phi(Q) \frac{\partial G(P, Q)}{\partial n_Q} - G(P, Q) \frac{\partial \phi(Q)}{\partial n_Q} \right] dS_Q = 0 \quad (8)$$

where  $\phi$  is the acoustic potential function and  $G$  is the Green's function defined by Eqs. (14-16), which also satisfies the Helmholtz equation. The Green's function is regular inside the surface except when  $P=Q$ . At this point  $G$  is singular. To remove this singularity from the integral given by Eq. (8), point  $P$  is surrounded by a small sphere or circle  $\sigma$  of radius  $\epsilon$ . The integral will now include a term over  $\sigma$  which, on taking the limit as  $\epsilon \rightarrow 0$ , gives

$$\phi(P) = C \int_{\Gamma} \left[ G(P, Q) \frac{\partial \phi(Q)}{\partial n_Q} - \phi(Q) \frac{\partial G(P, Q)}{\partial n_Q} \right] dS_Q \quad (9)$$

where  $C$  is  $i/4$  for two dimensions and  $1/4\pi$  for axisymmetric and three-dimensional shapes.

From Eq. (9) the value of the acoustic potential function at any point  $P$  within the surface can be determined from the boundary values of the potential and its normal derivative. Thus, the entire wave pattern within the surface can be constructed. For arbitrarily shaped surfaces for which numerical techniques must be used to obtain a solution, Eq. (9) requires much less computer storage than the differential

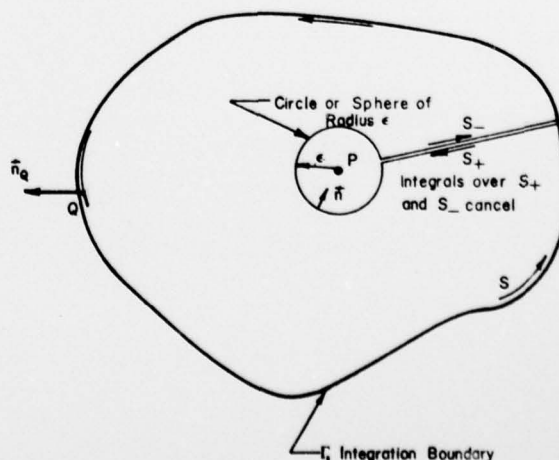


Fig. 1 Integration surface for an interior point.

formulation given by Eq. (7). Using Eq. (9) the value of the potential at each interior point can be obtained independently, whereas the method of finite differences used to solve Eq. (7) requires the simultaneous solution of  $\phi$  for every interior point. The integral formulation avoids the large matrices involved with finite differences.

If the values of both  $\phi$  and  $\partial\phi/\partial n$  are known at every point on the boundary then the wave pattern can readily be determined from Eq. (9). However, for most practical acoustic problems either  $\partial\phi/\partial n$  or an admittance condition relating  $\phi$  and  $\partial\phi/\partial n$  are given. Therefore, the values of the acoustic potential at the boundary must first be determined. The necessary relation is obtained by letting the point  $r$  approach the boundary at some point  $T$  to obtain the following relation<sup>26</sup>

$$\phi(T) = 2C \int_{\Gamma} [G(T, Q) \frac{\partial\phi(Q)}{\partial n_Q} - \phi(Q) \frac{\partial G(T, Q)}{\partial n_Q}] dS_Q \quad (10)$$

Eq. (10) is applicable to a smooth boundary, but has been extended to include cusps and corners.<sup>19,24</sup> To obtain the interior wave pattern, Eq. (10) is first solved for the boundary values of  $\phi$ . These values are then substituted into Eq. (9) to determine the acoustic potential at the interior points. Both Eqs. (9) and (10) involve singular integrands as  $T$  approaches  $Q$  although for smooth surfaces the integrals themselves are regular.

For exterior problems, analogous expressions to Eqs. (9) and (10) are obtained by taking the point  $P$  outside the surface  $\Gamma$ .<sup>4</sup> The integration in Eq. (8) is then carried out over the boundary, around a circle or sphere of radius  $\epsilon$  with point  $P$  as a center, and then around a circle or sphere of radius  $R$ , which is arbitrarily large. In this manner the integration includes the entire external domain. However, by applying Sommerfeld's radiation condition, it can be shown that the integral about the infinite sphere or circle approaches zero as  $R$  approaches infinity.<sup>4</sup> Thus, the corresponding equations for the external domain become

$$\phi(P) = -C \int_{\Gamma} [G(P, Q) \frac{\partial\phi(Q)}{\partial n_Q} - \phi(Q) \frac{\partial G(P, Q)}{\partial n_Q}] dS_Q \quad (11)$$

and

$$\phi(T) = -2C \int_{\Gamma} [G(T, Q) \frac{\partial\phi(Q)}{\partial n_Q} - \phi(Q) \frac{\partial G(T, Q)}{\partial n_Q}] dS_Q \quad (12)$$

It is important to note that Eqs. (11) and (12) involve integrations about the boundary of the body only. Thus, the radiated field at any distance from the body can be obtained once the surface acoustic potential is known. With finite differences, the values of the potential at every point in a very large domain would have to be computed in order to obtain the radiated field. Also, an artificial boundary condition at a large distance from the surface must be assumed. These factors make the application of finite differences to problems of this type rather inefficient whereas the integral formulation can readily be adopted to such situations.

Eqs. (9) through (12) are applicable to two-dimensional, axisymmetric, and three-dimensional acoustic problems. In the two-dimensional and axisymmetric cases, these equations involve line integrals; and in the three-dimensional case, the integrals are taken over a surface. Note that the dimensionality of the problem is reduced by one—a valuable simplification.

The Green's functions satisfy the following inhomogeneous forms of the Helmholtz reduction with homogeneous boundary conditions<sup>1</sup>

$$\nabla^2 G + k^2 G = \delta(P - Q) \quad (13)$$

where  $\delta$  is the Dirac delta function. The Green's functions are<sup>1,17,18</sup>

$$G(P, Q) = H_0^{(1)}(kr) \text{ for two dimensions,} \quad (14)$$

$$G(P, Q) = 2 \int_0^\pi \frac{e^{ikr}}{r} \cos m\theta d\theta \text{ for axisymmetric bodies} \quad (15)$$

and

$$G(P, Q) = e^{-ikr}/r \text{ for three dimensions} \quad (16)$$

where  $r$  is the distance between points  $P$  and  $Q$ , and  $H_0^{(1)}(kr)$  is the zeroth order Hankel function of the first kind.

#### Boundary Conditions

The two most common boundary conditions in practical acoustic problems are the Neumann and Robin conditions. The Neumann condition of interest in the present study is

$$\partial\phi/\partial n = A \quad (17)$$

where  $A$  is the velocity amplitude of a given sound source. In the absence of a sound source  $A = 0$ ; this condition means that the particle velocity is zero at the boundary which implies a perfectly reflecting, or rigid surface. For surfaces which absorb sound, such as lined duct walls, an admittance condition is usually specified, which leads to the Robin condition. Defined as the ratio of the normal component of the particle velocity to the pressure perturbation, the admittance  $y$  can be written as

$$y = \rho_0 c_0 (u_n / p) \quad (18)$$

Substituting for  $u_n$  and  $p$  from Eqs. (3) and (4) gives

$$(\partial\phi/\partial n) + iky\phi = 0 \quad (19)$$

Eq. (19) is the Robin condition.<sup>29</sup> For sound-absorbing materials or devices, the admittance can be either analytically determined<sup>30-32</sup> or measured using the impedance tube or a related technique.<sup>33-34</sup> The effects of a given material on the internal acoustic properties of a particular geometry can be

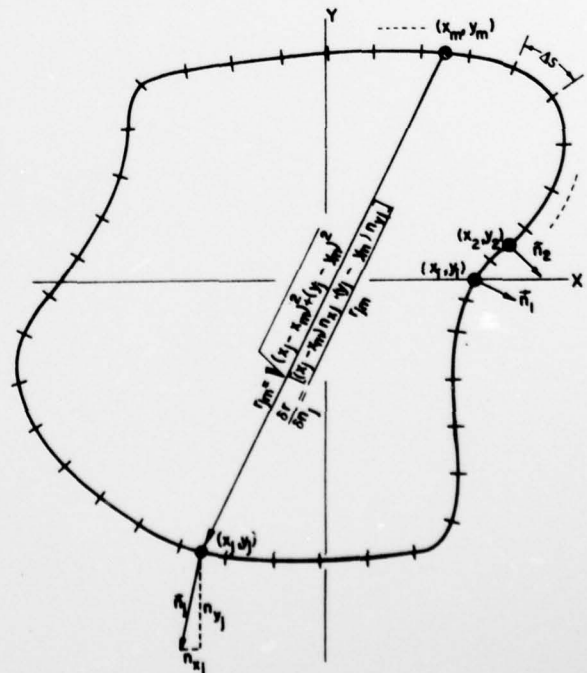


Fig. 2 Geometric considerations for the general problem.

determined by substituting the admittance of the material into Eq. (19) and solving Eqs. (9) and (10) or (11) and (12) for the acoustic potential. Thus, the analytical techniques used in this investigation is applicable to a vast number of duct acoustic problems. Since the admittance of a combustion process can also be measured,<sup>35</sup> this analysis can also be applied to related linear combustion instability problems, provided that the equations are applied to regions where the Helmholtz equation holds and mean flow effects can be neglected. By replacing the combustion process by an admittance condition, studies of combustion instability have been conducted in liquid and solid propellant combustors.<sup>36-37</sup> This research allows the extension of these analyses to more general shapes.

Substituting Eq. (19) into Eq. (10) gives for the internal field

$$\begin{aligned} \phi(T) + 2C \int_{\Gamma} \phi(Q) \left[ \frac{\partial G(T, Q)}{\partial n_Q} + iky(Q)G(T, Q) \right] dS_Q \\ = -2C \int_{\Gamma} A(Q)G(T, Q) dS_Q \end{aligned} \quad (20)$$

A similar expression is obtained from Eq. (12) for the exterior problem. For surfaces with spatially varying admittances, the admittance is a function of  $Q$ . For most cases considered in this study,  $y$  is assumed constant although nonuniform admittance distributions can be easily handled.

### III. Solution Technique

In the last section, the integral equations were developed which describe the interior and exterior acoustic fields or a surface with arbitrary shape and mixed boundary conditions. The numerical solution technique for solving these equations to obtain the internal or radiated acoustic patterns is presented in this section and can be divided into four parts. The first is the discretization of the integral equations into a corresponding system of linear, and algebraic equations in  $\phi$  suitable for solution on a computer. The second part is the specification of the geometry and boundary conditions. The third is the computation of the coefficients of the system of equations and the final part is the methods used to solve for the surface potential from the algebraic equations.

#### Discretization of the Integral Equations

In two dimensions and for axisymmetric problems, Eq. (20) involves a one-dimensional improper integral about the boundary line. For this type of problem several numerical integration techniques<sup>38-39</sup> are available. The simplest is the trapezoidal rule which has been shown to yield excellent results in two-dimensional studies with this type of integral.<sup>19,24,25</sup> Using this numerical integration scheme, Eq. (20) becomes

$$\begin{aligned} \phi_m + 2C \sum_{j=1}^N \phi_j \left[ \frac{\partial G(r_{jm})}{\partial n_j} + iky_j G(r_{jm}) \right] \Delta S_j \\ = -2C \sum_{j=1}^N A_j G(r_{jm}) \Delta S_j \end{aligned} \quad (21)$$

where one equation for  $\phi$  is obtained for each value of  $m$  and  $m$  is varied from 1 to  $N$ . Eq. (21) was initially used in this investigation to generate the  $N$  equations for  $\phi$  and accurate results were obtained when the admittance  $y$  was zero everywhere on the boundary<sup>40</sup> which is the case considered in previous studies.<sup>19,24,25</sup> However, when a nonzero admittance is assumed, this technique gives inaccurate results because of the contribution from the Green's function when the point  $j$  approaches  $m$ . Because of the singular nature of the Green's function at the point  $m$ , care must be taken when numerically integrating this function over the subinterval  $m$ . To increase the accuracy in evaluating the integrand, Eq. (20) is broken up into  $N$  integrals given by Eq. (22).

$$\begin{aligned} \phi_m \left\{ 1 + 2C \int_{S_{m-1/2}}^{S_{m+1/2}} \left[ \frac{\partial G(r_{1/2})}{\partial n_{1/2}} + iky_m G(r_{1/2}) \right] dS_j \right\} \\ + 2C \sum_{\substack{j=1 \\ j \neq m}}^N \phi_j \int_{S_{j-1/2}}^{S_{j+1/2}} \left[ \frac{\partial G(r_{jm})}{\partial n_j} + iky_j G(r_{jm}) \right] dS_j \\ = -2C \sum_{j=1}^N A_j \int_{S_{j-1/2}}^{S_{j+1/2}} G(r_{jm}) dS_j \end{aligned} \quad (22)$$

In both Eqs. (21) and (22) the values of  $\phi$  are assumed to be constant over each of the  $N$  subintervals. The difference is the method by which the terms involving the Green's function are evaluated. In Eq. (21) an average value is computed over each of the subintervals based on  $r_{jm}$ . With Eq. (22) these terms are integrated numerically from  $r_{j-1/2,m}$  to  $r_{j+1/2,m}$  using Gaussian quadrature<sup>39,40</sup> to obtain more accurate values. This type of formulation has been used before with trapezoidal instead of Gaussian quadrature formulas.<sup>18</sup> In the present study for two-dimensional and axisymmetric problems, a reduction in error of two orders of magnitude in the numerical results for a nonzero admittance was achieved using Eq. (22) instead of Eq. (21).<sup>40</sup>

#### Surface Geometry and Boundary Conditions

The first step in solving Eq. (22) is the determination of the coefficients of  $\phi_j$  and  $\phi_m$ . These coefficients depend upon the surface geometry through the terms  $\partial/\partial n_j$ ,  $r_{jm}$ , and  $\Delta S_j$ . By specifying the admittance  $y$  and/or the sound velocity amplitude  $A$  over every subinterval  $j$ , the effect of the boundary conditions are included in the evaluation of the coefficients.

To solve for the terms involving the surface geometry, the first expression inside the integrals of Eq. (22) is written as

$$\frac{\partial G(r)}{\partial n} = \frac{\partial G(r)}{\partial r} \frac{\partial r}{\partial n}$$

The expressions for  $\partial G/\partial r$  are obtained by differentiating Eqs. (14) through (16). Substituting this expression into Eq. (22)

Table 1 Eigenfrequencies and natural modes of a circle for various admittance values






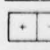

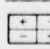
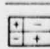
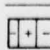
MODE		ADMITTANCE VALUE		
		$y = 0$	$y = 0.3$	$y = 0.3i$
	COMPUTED	1.84122	1.8324 + 0.4423i	1.4441 - 0.0071i
	EXACT	1.84116	1.8322 + 0.4432i	1.4384
	COMPUTED	3.05423	3.0791 + 0.5397i	2.5369 - 0.0151i
	EXACT	3.05424	3.0786 + 0.5442i	2.5427
	COMPUTED	3.83175	Not Computed	Not Computed
	EXACT	3.83171	3.8188 + 0.3095i	3.5510
	COMPUTED	4.20135	4.2538 0.6199i	3.5816 - 0.0231i
	EXACT	4.20119	4.2532 0.6351i	3.5615
	COMPUTED	5.31783	Not Computed	Not Computed
	EXACT	5.31755	5.3953 0.7101i	4.5767

Table 2 Resonant frequencies and natural modes of a rectangle for different admittance values at the ends

MODE		ADMITTANCE VALUE		
		$y = 0$	$y = 0.3$	$y = 0.3i$
	COMPUTED	3.1432	3.150 + 0.6199i	2.558 + 0.0021i
	EXACT	3.1416	3.142 + 0.6190i	2.559
	COMPUTED	6.2877	6.302 + 0.6156i	5.886 + 0.0021i
	EXACT	6.2832	6.283 + 0.6190i	5.884
	COMPUTED	7.0312	7.146 + 0.5881i	6.333 - 0.007i
	EXACT	7.0248	Not Computed	6.283
	COMPUTED	8.893	8.934 + 0.6101i	8.303 - 0.0111i
	EXACT	8.886	Not Computed	8.299
	COMPUTED	9.4329	9.456 + 0.6106i	8.847 + 0.0071i
	EXACT	9.4248	9.425 + 0.6190i	8.8421

gives a relation which involves  $\partial r/\partial n_j$ ,  $r_{jm}$  and  $dS$ . The expressions for  $\partial r/\partial n_j$ ,  $r_{jm}$  and  $dS$  can be written in parametric form for bodies with simple shapes, and this type of representation has been used in previous studies using simple geometries.<sup>19,20,24,41,42</sup> By taking advantage of symmetry, considerable savings in computer storage and computation times were achieved. In fact, Greenspan and Werner<sup>42</sup> showed that for a circle, Eq. (22) can be reduced to a single equation instead of a system of equations which could readily be solved to obtain the acoustic field. In the study by Tai and Shaw,<sup>25</sup> the method of images (Ref. 1, Ch. 11) was used to greatly reduce the number of points necessary to compute eigenfrequencies and eigenmodes of a family of triangles. Although these studies demonstrate valuable simplifications which can be made in applying the integral formulation to a particular problem, the techniques used are not applicable to more general problems involving complicated geometries and nonuniform boundary conditions.

In the present study for two dimensions, the expressions for the geometric variables are written in parametric form only for the circle. In the rest of the configurations considered, a general formulation is used. The fact that a parametric representation cannot be used in general cases is not a serious drawback—in fact, it somewhat simplifies the formulation. Consider the general two-dimensional problem depicted in Fig. 2. By specifying the  $x$  and  $y$  coordinates at the midpoint of each of the subintervals, the distance  $r_{jm}$  is readily computed from the expression

$$r_{jm} = \sqrt{(x_j - x_m)^2 + (y_j - y_m)^2} \quad (23)$$

The expression for  $\partial r/\partial n_j$  can then be obtained since it represents the dot product of the gradient of  $r$  and the normal at  $j$ . Thus,

$$\frac{\partial r}{\partial n_j} = \frac{(x_j - x_m)n_{xj} + (y_j - y_m)n_{yj}}{r_{jm}} \quad (24)$$

where  $n_{xj}$  is the component of the normal vector  $j$  in the  $x$  direction (or the cosine of the angle between the normal vector and the  $x$ -axis) and  $n_{yj}$  is the corresponding  $y$  component (the sine of the angle between the normal vector and the  $y$ -axis). Analogous expressions for  $r_{jm}$  and  $\partial r/\partial n_j$  can be obtained for axisymmetric<sup>17,18</sup> and three-dimensional problems. For two-dimensional and axisymmetric problems, the line segment length  $\Delta S_j$  is simply

$$\Delta S_j = \sqrt{(x_{j+1} - x_{j-1})^2 + (y_{j+1} - y_{j-1})^2}$$

or, for  $N$  equally spaced subintervals,  $S_j = L/N$  where  $L$  is the length of the perimeter of the surface. For three-dimensional bodies,  $\Delta S_j$  is the area of each of the subsurfaces taken over the boundary.

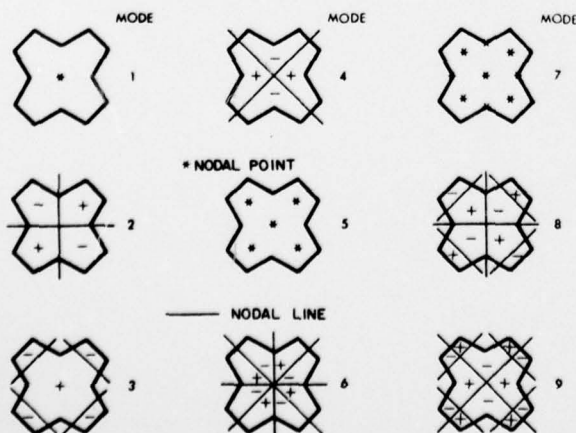


Fig. 3 Nodal points and lines for the first nine modes of the star.

#### Computation of the Coefficients of the Discretized Integral Equation

Once the geometry has been specified, the coefficient of  $\phi$  in Eq. (22) can be determined by evaluating the Green's functions  $G(r_{jm})$  and  $\partial G(r_{jm})/\partial r_{jm}$ . There are two problems in determining these functions: the first is a rapid, accurate method for computing them over a wide range of the argument  $kr_{jm}$ ; and the second is the singularity associated with each function as  $r_{jm}$  approaches zero.

For the two-dimensional problems to compute the Hankel functions two routines have been used in this study. The first consists of a series expansion using standard formulas for the Hankel function with complex arguments.<sup>39,43</sup> A sufficient number of terms is taken to satisfy a specified degree of accuracy. To minimize time, a different series expansion which was developed by Hitchcock<sup>44</sup> is used for determining these functions in the studies of the rectangle, star, and duct with a right-angle bend. With his formulation, accuracies of  $10^{-10}$  or greater are achieved using nine terms or less in the series expansion. Reductions of up to 50% in computer times can be achieved with this formulation.

For the axisymmetric problem, the integral in Eq. (15) is carried out using a 20-point Gauss-Legendre quadrature formula. For three-dimensional problems, evaluation of the Green's function given by Eq. (16) is straightforward.

The major problem in accurately computing the coefficients in Eq. (22) is the singularity associated with the Green's functions as  $r_{jm}$  approaches zero; that is, as the point  $j$  approaches  $m$  in Fig. 2. The two-dimensional and axisymmetric Green's functions have logarithmic singularities. In this study, the inaccuracies involved are minimized by subdividing the intervals as indicated by Eq. (22).

#### Determination of the Acoustic Potential

Once the coefficients of the surface potential at each discrete point on the surface are determined, the equations are solved for  $\phi$  using a complex Gauss-Jordan reduction scheme. The interior or exterior points can then be found using the discretized form of Eq. (9).

To determine the eigenfrequencies of a particular geometry, the technique described in Ref. 40 is used. Essentially, this technique consists of: 1) determining the frequency  $k$  for which the determinant of the coefficients in the homogeneous form of Eq. (22) is zero, 2) normalizing the equation at the eigenfrequency to obtain the surface distribution of the mode, and 3) using Eq. (9) in discretized form to find the interior sound field.

#### V. Results

Using the numerical techniques described in the last section, solutions have been obtained for a variety of two-dimensional and axisymmetric problems to demonstrate its broad range of

Table 3 Surface potentials for a circle of unit radius, second mode,  $V=0$

Angle	Numerical	Exact
12	.9130	.9135
24	.6681	.6691
36	.3077	.3090
48	-.1059	-.1045
60	-.5012	-.5000
72	-.8099	-.8090
84	-.9785	-.9781
96	-.9779	-.9781
108	-.8082	-.8090
120	-.4988	-.5000
132	-.1013	-.1045
144	.3104	.3090
156	.6702	.6691
168	.9141	.9135
180	1.0000	1.0000

Table 4 Surface potential for a rectangle, height to width ratio = 0.5, first mode, rigid walls

	Y	Numerical	Exact
1/2	1/14	1.0061	1.0063
1/2	2/14	1.0060	1.0063
1/2	3/14	1.0055	1.0063
13/28	1/4	1.0000	1.0000
11/28	1/4	.9501	.9499
9/28	1/4	.8524	.8521
7/28	1/4	.7119	.7116
5/28	1/4	.5356	.5354
3/28	1/4	.3325	.3324
1/28	1/4	.1127	.1127

applications. The two-dimensional form of the integral equation has been used to compute the resonant frequencies and natural modes of a circle, rectangle, and star configuration. In addition, the problem of a duct with a right angle bend is considered, and results using Eq. (22) are compared with finite difference solutions. The two-dimensional problem of sound radiation from a right circular cylinder is then considered and the numerical and exact solutions are compared. Finally the acoustic properties of a sphere are computed using the axisymmetric formulation.

For a circle and rectangle, comparisons between exact and numerical solutions are presented in Tables 1 and 2. In these tables the numerical and exact eigenfrequencies are tabulated for three admittance values,  $y=0$ ,  $y=0.3$ ,  $y=0.3i$ , with thirty points taken on the boundary. The best agreement between the computed and exact results occurs at the zero admittance condition. For the circle, the real part of the eigenfrequencies compare to five significant figures and the imaginary parts are accurate to 0.001 for the first five modes. When a nonzero admittance condition is introduced, the accuracy is reduced to three significant figures in the real part and to 0.01 in the imaginary part of the eigenfrequencies.

As with the circle, the agreement between the exact and numerical values for the rectangle is good for a rigid boundary but deteriorates when a nonzero admittance is introduced. From Table 2 the agreement is to almost four significant figures in the real part of the eigenfrequency and to within 0.01 in the imaginary part for a rigid wall. The Gaussian integration techniques developed in Sec. III improve

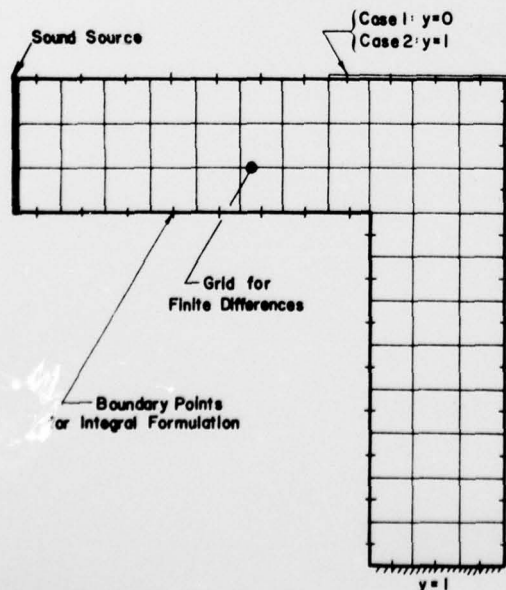


Fig. 4 Locations of the discrete points, nonzero admittance boundaries, and the sound source for the duct with a right-angle bend.

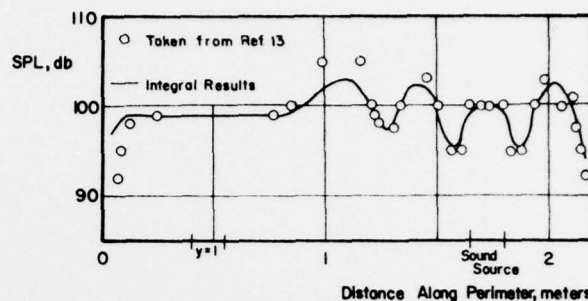


Fig. 5 Comparison of numerical results for a duct with a right-angle bend using the integral and finite difference approaches, Case 1.

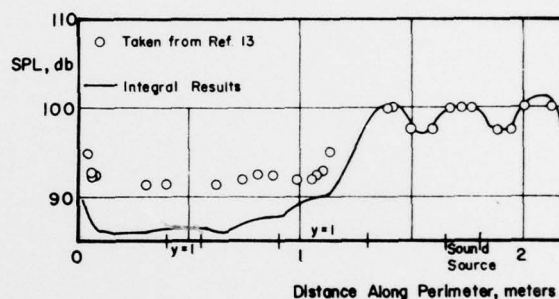


Fig. 6 Comparison of numerical results for a duct with a right-angle bend using the integral and finite difference approaches, Case 2.

the accuracy of the computed eigenfrequencies for a nonzero admittance condition by an order of magnitude.

For the circle the accuracy of the computed natural mode shapes is shown in Table 3. The agreement between the exact and computed eigenmodes for a rigid boundary is to within 0.01% for interior points sufficiently far removed from the boundary. For a nonzero admittance at the surface, the accuracy is to within 2%. These results are obtained using the interior analog of Eq. (21) which explains the deterioration in accuracy of the interior points as the boundary is approached. Equation (22) is used in the studies of the rectangle, star, and duct problems and more accurate results are obtained close to the boundary. For the rectangle, the boundary values of the acoustic potential are presented in Table 4. The agreement between the exact and numerical results is within one-half of a percent. Computation times range from ten sec per eigenfrequency for the circle to 45 sec for the rectangle on UNIVAC 1108 computer. Using the discretized form of Eq. (9), interior points require approximately two sec per point to compute.

In studying the star-shaped boundary, which is of interest in solid-rocket combustion instability problems, the applicability of the integral solution technique to a complicated geometry for which separation of variables does not apply can be assessed. The first nine eigenfrequencies and natural modes for the star are presented in Fig. 3 for a rigid wall with 48 points taken on the surface. The most unique feature of the acoustic field for the star is the appearance of nodal points at some of the resonant modes. In the circle and rectangle nodal lines only are present, and they follow one of the separable coordinates of the boundary. With the star both nodal lines and points can occur which is in qualitative agreement with experimental observations for unstable solid propellant combustors. Computation times are from 60 to 75 sec per mode. The modes of a typical solid propellant configuration during a burn have also been computed and are given in Ref. 45.

The last internal two-dimensional problem investigated is that of a duct with a right-angle bend shown in Fig. 4. The reasons for studying this configuration are: 1) to investigate a

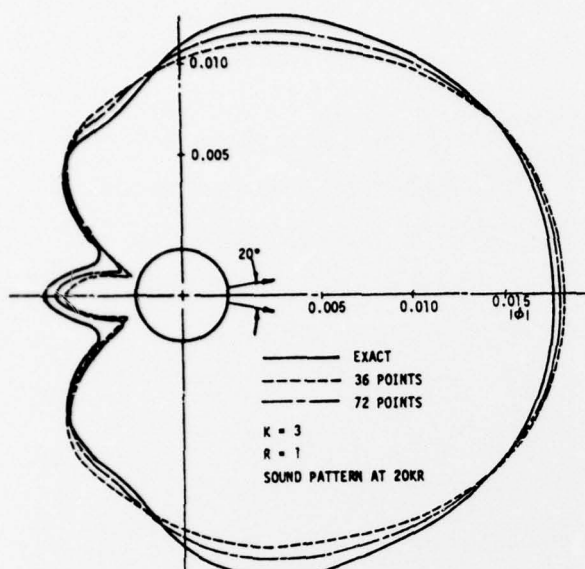


Fig. 7 Sound pattern produced by a 20° vibrating piston set in a circular cylinder.

nonuniform surface admittance, 2) to include a sound source in the integral formulation, and 3) compare the results obtained by the integral technique with the finite difference solutions of Ref. 13.

The results obtained using this configuration are presented in Figs. 5 and 6 and are compared with the solutions obtained using the finite difference method. Although the results using the integral approach are in qualitative agreement with the finite difference solution, quantitative agreement is lacking. The same number of boundary points are taken in both cases. Doubling the number of subintervals using Eq. (22) does not improve the agreement between the two sets of data. However, it does show that the results of the integral formulation are self-consistent. An experimental setup is

Table 5 Resonant frequencies and surface potentials for a sphere of unit radius, first and second modes, axisymmetric formulation

Resonant frequencies		
Computed		Exact
2.084-0.0041		2.082
3.346-0.0071		3.342
Normalized surface potential		
Angle	Computed	Exact
(First mode)		
5	1.00000	1.00000
15	.96960	.96962
25	.90975	.90977
35	.82232	.82228
45	.70992	.70981
55	.57593	.57577
65	.42439	.42423
75	.25992	.25981
85	.08753	.08749
(Second mode)		
5	1.0000	1.0000
15	.9098	.9099
25	.7403	.7405
35	.5121	.5124
45	.2275	.2529
55	-.0072	-.0066
65	-.2346	-.2348
75	-.4051	-.4041
85	-.4953	-.4942

<sup>a</sup>Numerical results obtained using Eq. (21) instead of Eq. (22).

currently being developed to check these results and should clarify the discrepancy between these two methods.

For two-dimensional radiation problems, excellent results are obtained as shown in Fig. 7. Here the radiated field from a piston set in a right circular cylinder is computed and compared with exact results from Ref. 3. The mean square error is less than 2% while the computation time required is 15 sec to obtain both the surface and far field patterns.

To check the accuracy of the axisymmetric formulation, the first two resonant frequencies and natural mode shapes of a sphere were computed and are presented in Table 5. As with the two-dimensional problems, agreement between the exact and numerical calculations is excellent. Computation times are approximately two minutes per mode; however, no attempt was made to take advantage of the symmetry of the problem which can reduce the computation time by at least a factor of two.

### Conclusions and Recommendations

The results for the circle and rectangle show that the integral technique is very accurate in determining resonant frequencies and natural mode shapes. Its application to the star configuration demonstrates its usefulness in studying the acoustics of complicated shapes. For the duct with a right-angle bend, the integral approach is shown to be applicable to nonuniform boundary conditions involving sound sources. The formulation also gives accurate results for two-dimensional radiation problems shown in the study of the right circular cylinder.

With the axisymmetric formulation accurate results are obtained for the internal eigenmodes of a sphere. Extensions to more complicated boundaries can readily be made.

### Acknowledgment

Most of this work was conducted under NSF Research Initiation Grant GK-42159.

### References

- <sup>1</sup>Morse, P. M. and Feshbach, H., *Methods of Theoretical Physics, Parts I and II*, McGraw-Hill, New York, 1953.
- <sup>2</sup>Weinberger, H. F., *A First Course in Partial Differential Equations*, Blaisdell, Waltham, Mass., 1965.
- <sup>3</sup>Morse, P. M. and Ingard, K. U., Ch. 9, *Theoretical Acoustics*, McGraw-Hill, New York, 1969.
- <sup>4</sup>Skudrzyk, E., *The Foundations of Acoustics*, Springer-Verlag, Vienna, Austria, 1971, Ch. 22 and 23.
- <sup>5</sup>Mitchell, C. E., Espander, W. R., and Baer, M. R., "Determination of Decay Coefficients for Combustors with Acoustic Absorbers," NASA CR 120836, Jan. 1972.
- <sup>6</sup>Oberg, C. L., "Improved Design Techniques for Acoustic Liners," Rocketdyne, Canoga Park, Calif., Report No. RR-68-5, May 1968.
- <sup>7</sup>Oberg, C. L., Wong, T. L., and Schmeltzer, R. A., "Analysis of the Acoustic Behavior of the Baffled Combustion Chambers," NASA CR 72625, Jan. 1970.
- <sup>8</sup>Doak, P. E., "Excitation, Transmission and Radiation of Sound from Source Distributions in Hard-Walled Ducts of Finite Length (I): The Effects of Duct Cross-Section Geometry and Source Distribution Space-Time Pattern, (II): The Effect of Duct Length," *Journal of Sound and Vibration*, Vol. 31, Jan. 1973, pp. 1-72, and Feb. 1973, pp. 137-174.
- <sup>9</sup>Lansing, D. L. and Zorumski, W. E., "Effects of Wall Admittance Changes on Duct Transmission and Radiation of Sound," *Journal of Sound and Vibration*, Vol. 27, Jan. 1973, pp. 85-100.
- <sup>10</sup>Wynne, G. A. and Plumblee, H. E., "Calculation of Eigenvalues of the Finite Difference Equations Describing Sound Propagation in a Duct Carrying Shear Flow," presented at the 79th Meeting of the Acoustical Society of America, Atlantic City, N.J., April 21, 1970.
- <sup>11</sup>Baumeister, K. J., "Application of Finite Difference Techniques to Noise Propagation in Jet Engines," NASA TMX-68621, Nov. 1973.
- <sup>12</sup>Baumeister, K. J. and Rice, E. J., "A Difference Theory for Noise Propagation in an Acoustically Lined Duct with Mean Flow," *AIAA Progress in Astronautics and Aeronautics: Aeroacoustics: Jet*

and Combustion Noise, Vol. 37, Editor: Henry T. Nagamatsu; Associate Editors: Jack V. O'Keefe and Ira R. Schwartz, MIT Press, Cambridge, Mass., 1975, pp. 435-453.

<sup>13</sup>Alfredson, R. J., "A Note on the Use of the Finite Difference Method for Predicting Steady State Sound Fields," *Acustica*, Vol. 28, May 1973, 296-301.

<sup>14</sup>Cantin, G., "Three-Dimensional Finite Element Studies, Part One: Service Routines," Naval Postgraduate School, Monterey, Calif., NPS-59C 172121A, Dec. 1972.

<sup>15</sup>Chen, L. H. and Schweikert, D. G., "Sound Radiation from an Arbitrary Body," *Journal of the Acoustical Society of America*, Vol. 35, Oct. 1963, pp. 1626-1632.

<sup>16</sup>Chen, L. H., "A Matrix Method of Analysis of Structure-Fluid Interaction Problems," ASME Paper 61-WA-220, Aug. 1961.

<sup>17</sup>Chertock, G., "Sound from Vibrating Surfaces," *Journal of the Acoustical Society of America*, Vol. 36, July 1964, pp. 1305-1313.

<sup>18</sup>Copley, L. G., "Integral Equation Method for Radiation from Vibrating Bodies," *Journal of the Acoustical Society of America*, Vol. 42, April 1967, pp. 807-816.

<sup>19</sup>Banaugh, R. P. and Goldsmith, W., "Diffraction of Steady Acoustic Waves by Surfaces of Arbitrary Shape," *Journal of the Acoustical Society of America*, Vol. 35, Oct. 1963, pp. 1590-1601.

<sup>20</sup>Mitzner, K. M., "Numerical Solution for Transient Scattering from a Hard Surface of Arbitrary Shape-Retarded Potential Technique," *Journal of the Acoustical Society of America*, Vol. 42, Feb. 1967, pp. 391-397.

<sup>21</sup>Shaw, R. P., "Scattering of Plane Acoustic Pulses by an Infinite Plane with a General First-Order Boundary Condition," *Journal of Applied Mechanics*, Sept. 1967, pp. 770-772.

<sup>22</sup>Quinn, D. W., "An Integral Equation Method for Duct Acoustics with Varying Cross Sections and Axially Varying Impedance," *AIAA Journal*, Vol. 15, Feb. 1977, pp. 278-281.

<sup>23</sup>Liu, H. K. and Martenson, A. J., "Optimum Lining Configurations," *Basic Aerodynamic Noise Research*, NASA SP-207, July 1969, pp. 425-434.

<sup>24</sup>Zinn, B. T. and Gaylord, C. G., Unpublished Notes and "An Analytical Investigation of Acoustic Modes of Two and Three Dimensional Solid Rocket Motors," a Thesis Proposal by C. G. Gaylord, School of A. E., Georgia Tech., Atlanta, Ga.

<sup>25</sup>Tai, G. C. and Shaw, R. P., "Eigenvalues and Eigenmodes for the Homogeneous Helmholtz Equation for Arbitrary Domains," Report No. 90, Dept. of E. S., State University of N.Y. at Buffalo, Aug. 1973.

<sup>26</sup>Kellogg, O. D., Ch. VI, *Foundations of Potential Theory*, Dover Publications, New York, 1953.

<sup>27</sup>Webster, A. G., Ch. VIII, *The Dynamics of Particles*, Dover Publications, New York, 1959.

<sup>28</sup>Baker, B. B. and Copson, E. T., Ch. I, *The Mathematical Theory of Huygens' Principle*, Oxford at the Clarendon Press, 1950.

<sup>29</sup>Burton, A. J., "The Solution of Helmholtz's Equation in Exterior Domains Using Integral Equations," NPL Report NAC 30, National Physical Laboratory, Teddington, Middlesex, Jan. 1973.

<sup>30</sup>Strutt, J. W. (Lord Rayleigh), Ch. 16, *The Theory of Sound*, Vol. II, Dover Publications, New York, 1945.

<sup>31</sup>Ingard, K. U., "On the Theory and Design of Acoustic Resonators," *Journal of the Acoustical Society of America*, Vol. 25, Nov. 1953, pp. 1037-1061.

<sup>32</sup>Crocco, L. and Sirignano, W. A., "Behavior of Supercritical Nozzles under Three-Dimensional Oscillatory Conditions," AGARDograph 117, Butterworth Publications, London, 1967.

<sup>33</sup>Scott, R. A., "An Apparatus for Accurate Measurement of the Acoustic Impedance of Sound Absorbing Materials," *Proceedings of the Physical Society*, Vol. 58, 1946, p. 253.

<sup>34</sup>Zinn, B. T., Bell, W. A., and Daniel, B. R., "Experimental Determination of Three-Dimensional Liquid Nozzle Admittances," *AIAA Journal*, Vol. 11, March 1973, pp. 267-272.

<sup>35</sup>*T-Burner Manual*, Chemical Propulsion Information Agency, CPIA Publication No. 191, Nov. 1969.

<sup>36</sup>Crocco, L. and Cheng, S. I., "Theory of Combustion Instability in Liquid Propellant Rocket Motors," AGARDograph 8, Butterworth Publications, London, 1956.

<sup>37</sup>Culick, F. E. C., "Review of Calculations for Unsteady Burning of a Solid Propellant," *AIAA Journal*, Vol. 6, Dec. 1968, pp. 2241-2255.

<sup>38</sup>Conte, S. D., Chs. 2 and 5, *Elementary Numerical Analysis*, McGraw-Hill, St. Louis, 1965.

<sup>39</sup>Abramowitz, M. and Stegun, I. A., *Handbook of Mathematical Functions*, NBS AMS No. 55, May 1968.

<sup>40</sup>Bell, W. A., "Resonant Frequencies and Natural Modes of Arbitrarily Shaped Ducts," Final Report, NSF Research Initiation Grant GK-42159, Georgia Tech., Atlanta, Ga., April 1, 1976.

<sup>41</sup>Jones, D. S., "Integral Equations for the Exterior Acoustic Problem," *Quarterly Journal of Mechanics & Applied Mathematics*, Vol. 27, Jan. 1974, pp. 129-142.

<sup>42</sup>Greenspan, D. and Werner, P., "A Numerical Method for the Exterior Dirichlet Problem for the Reduced Wave Equation," *Archive for Rational Mechanics and Analysis*, Vol. 23, No. 4, 1966, pp. 288-316.

<sup>43</sup>Gradshteyn, I. S. and Ryzhik, I. M., *Table of Integrals, Series, and Products*, Sixth Printing, Academic Press, New York, 1972, 951.

<sup>44</sup>Hitchcock, A. J. M., "Polynomial Approximations to Bessel Functions of Order Zero and One and to Related Functions," *Math Tables & Other Aids to Computations*, Vol. 11, 1957, pp. 86-88.

<sup>45</sup>Bell, W. A., Meyer, W. L., and Zinn, B. T., "Prediction of the Acoustics of Solid Propellant Rocket Combustors by Integral Techniques," *Proceedings of the 12th JANNAF Meeting*, CPIA Publications No. 273, Vol. II, 1975, pp. 19-33.

SECURITY CLASSIFICATION OF THIS PAGE (When Data Entered)

1. REPORT DOCUMENTATION PAGE		READ INSTRUCTIONS BEFORE COMPLETING FORM	
1. REPORT NUMBER AFOSR/TR-78-0696	2. GOVT ACCESSION NO.	3. RECIPIENT'S CATALOG NUMBER Scientific	
4. TITLE (and Subtitle) NOISE SUPPRESSION IN JET INLETS.	5. TYPE OF REPORT & PERIOD COVERED INTERIM rept. 1 Feb 77 - 31 Jan 78.		
7. AUTHOR(s) BEN T. ZINN, WILLIAM L. MEYER WILLIAM A. BELL	8. CONTRACT OR GRANT NUMBER(s) F49620-77-C-0066		
9. PERFORMING ORGANIZATION NAME AND ADDRESS GEORGIA INSTITUTE OF TECHNOLOGY SCHOOL OF AEROSPACE ENGINEERING ATLANTA, GEORGIA 30332	10. PROGRAM ELEMENT, PROJECT, TASK AREA & WORK UNIT NUMBERS 2307A2 61102F		
11. CONTROLLING OFFICE NAME AND ADDRESS AIR FORCE OFFICE OF SCIENTIFIC RESEARCH/NA BLDG 410 BOLLING AIR FORCE BASE, D C 20332	12. REPORT DATE Feb 78		
14. MONITORING AGENCY NAME & ADDRESS (if different from Controlling Office)	13. NUMBER OF PAGES 73		
	15. SECURITY CLASS. (of this report) UNCLASSIFIED		
15a. DECLASSIFICATION/DOWNGRADING SCHEDULE			
16. DISTRIBUTION STATEMENT (of this Report)  Approved for public release; distribution unlimited.			
17. DISTRIBUTION STATEMENT (of the abstract entered in Block 20, if different from Report)			
18. SUPPLEMENTARY NOTES			
19. KEY WORDS (Continue on reverse side if necessary and identify by block number) ACOUSTIC RADIATION DUCT ACOUSTICS JET PROPULSION NOISE AIRCRAFT NOISE			
20. ABSTRACT (Continue on reverse side if necessary and identify by block number) This report summarizes the work performed during the first year of a research effort to determine the sound fields associated with jet engine inlet configurations. A solution approach for axisymmetric bodies based upon the integral formulation of the wave equation has been developed. This solution approach circumvents the uniqueness problems which normally occur at certain frequencies when "straight forward" solutions of the integral equation are obtained. A numerical method and a computer program for solving for the acoustic field associated with general inlet configurations and boundary conditions have also been developed. To evaluate the numerical method, computed and exact results are			

DD FORM 1 JAN 73 1473

EDITION OF 1 NOV 65 IS OBSOLETE

UNCLASSIFIED

SECURITY CLASSIFICATION OF THIS PAGE (When Data Entered)

403 914

UNCLASSIFIED

SECURITY CLASSIFICATION OF THIS PAGE (When Data Entered)

compared for a sphere and a finite length cylinder. For continuous boundary conditions, the agreement is within ten per cent over a range of nondimensional frequencies from one to ten. For discontinuous boundary conditions, the numerical errors increase by a factor of two. This report presents results for a given inlet configuration and the computed and exact solutions are shown to agree to within ten per cent over the non-dimensional frequency range from one to ten.

UNCLASSIFIED